DEVELOPMENT OF A PARALLEL-PLATE IONIZATION CHAMBER FOR α-PARTICLES, AND ITS APPLICATION TO THE MEASUREMENT OF FLUORESCENCE YIELDS.

THESIS

submitted by

JACOB JAE HANG PARK, B.Sc.

for the degree of

DOCTOR OF PHILOSOPHY.

University of Edinburgh

October 1959.

PREFACE

The research described in this thesis was carried out in the Department of Natural Philosophy of the University of Edinburgh under the joint supervision of Professor N. Feather, F.R.S., Dr. M.A.S. Ross, and Dr. J. Muir.

A paper, based on a part of the results to be described below, has been presented at the Physical Society Conference on Nuclear Physics held at the University of Edinburgh on the 15th of September, 1959.

.....

CONTENTS

CONTENTS (Contd.)

CHAPTER I

INTRODUCTION.

General

When an atom is ionized in an inner shell, it may discharge its excess energy in the form of X-rays and the fraction of ionized atoms which so reorganize is termed the fluorescence yield, ω , for the shell in which the initial vacancy occurred. This phenomenon has been extensively studied since the early years of the present century (e.g. Barkla and Sadler, 1909, Beatty, 1911) and though it soon became clear that the emission of X-rays was not the only process whereby an ionized atom could emit its excess energy, it was not until 1925 that Auger showed that an alternative process was available, in the successive ejection of electrons from outer shells. The fraction of atoms which reorganize in this fashion is termed the Auger yield, a , and since the sum of the two yields is unity a measurement of one uniquely determines the other.

The fluorescence yield is of interest not only for the detailed interpretation of X-ray spectra but also for the elucidation of many problems arising in the field of radioactivity. The most extensive investigations made have been connected with the K shell fluorescence yield, ω_k , for which data are now available

for practically every element. Much less information has been obtained on the L shell fluorescence yield where the situation is complicated by the appearance of other phenomena and also by the fact that ω_L itself is a function of the method of producing the initial ionization. It is with the L-shell fluorescence yield that this thesis is chiefly concerned.

In discussing the experimental work which has been performed on the topic of fluorescence yields we may conveniently divide the experiments into two groups depending on whether the observations have been made on the X-rays or on the Auger electrons. Although the bulk of the information available has been obtained by the direct observation of the fluorescence yield nevertheless a greater variety of methods for measuring the Auger yield has appeared corresponding to the greater number of methods available for detecting and measuring electrons as opposed to X-rays.

One of the earliest and most direct methods for measuring the fraction of atoms reorganizing with the emission of electrons, consisted in counting the number of paired tracks appearing in cloud-chamber photographs of the type studied by Auger (1925) in his original discovery of the Auger effect. The initial excitation of the gaseous atoms was made using a collimated beam of X-rays, and comparison of the number of paired tracks and ordinary photoelectron tracks gave the desired information.

A method similar in principle is the photographic emulsion technique as used by Germain (1950) to measure the fluorescence yield of Po^{211}, by impregnating the photographic plates with At^{211}. 60 % of At^{211} decays to Po^{211} by electron capture with a half-life of 7.5 hours, while Po^{211} decays to Pb^{207} by α-disintegration with a half-life of (5×10^{-3} sec.). Since the α-decay of Po^{211} occurs with such a short half-life, any electron capture is followed immediately by an α-particle from Po^{211}. The origins of α-particle tracks in the emulsion locate the Po^{211} atoms ionized in an inner shell and by counting the number of Po^{211} α-tracks and the number of tracks which have at their origins an electron track of energy corresponding to a K-Auger electron it is possible to estimate the proportion of atoms that have reorganized by an Auger process. The tracks of the remaining 40 % of At^{211}, which decays by α-disintegration to Bi^{207}, can be distinguished by the range difference, and the correction due to L-capture applied.

Fluorescent yields may also be obtained for gases by using a proportional counter for electron detection and measurement (Curran, Angus and Cockroft, 1949, and West and Rothwell, 1950). When an exciting X-ray is absorbed by the K-shell of the counter gas and the atom reorganizes by means of an Auger transition, the full energy E of the incident X-radiation is dissipated

in the counter. When the atom reorganizes with the emission of K series X-radiation, however, a large proportion of the radiation will escape from the counter provided the pressure in it is not too high. The K-shell fluorescence yield of the counter gas is determined from the relative intensities of the two peaks in the pulse height distribution, one caused by the photoelectron alone and the other by the photoelectron accompanied by an Auger electron. This method has been extended to the solid material by Harrison et al. (1955) using radioactive sources of Zn^{65} and Sn^{113}. Zn^{65} decays to Cu^{65} by electron capture and positron emission (EC 98.5%, β^+ 1.5%) with a half-life of 245 days. Cu^{65} atoms with a vacancy in the K-shell reorganize either by X-ray or Auger electron emission producing two peaks in the pulse-height spectrum of 8 keV and 6.8 keV corresponding to the energies of the K X-rays and the K Auger electrons. By correcting for the counter efficiencies for the K X-ray and Auger electrons, the K-shell fluorescence yield of Cu^{65} is obtained.

Another method of measuring the fluorescence yield of a gas, observing the change of ionization at the critical frequency, is that first used by Martin (1927). The principle of the method is as follows. An ionization chamber is filled with the gas under investigation, and when a parallel beam of X-rays of known intensity is passed through the ionization chamber, the ionization

current can be calculated with a knowledge of the absorption jump ratio and the absorption coefficients just above and below the K critical frequency. An observation of the ionization at a frequency just above the critical frequency, which exceeds the calculated ionization due to the Auger electrons, gives a measure of the Auger effect. An assumption has been made here that all the K X-rays produced by the gas escape from the chamber.

The magnetic spectrometer has also been employed in the measurement of fluorescence yields of elements of high atomic number (Bergstrom and Thulin, 1950 ; Broyles et al., 1953). In this case the result is obtained by a direct comparison of the intensities of Auger and conversion electrons following the internal conversion of a γ -ray.

If the reorganization process is studied by measuring the intensity of the characteristic radiation rather than that of the Auger electrons, the most direct method consists in the use of an ionization chamber to compare the ionization current due to the fluorescent radiation with the ionization current due to the exciting beam. Most of the early results on the fluorescent yields have been obtained by this method.

The solid angle difference method was first introduced by Roos (1954), who used an NaI (Tl) crystal scintillation counter to detect the X-rays. The sample

in the form of a foil was pressed in contact with the NaI (Tl) crystal so that the fluorescent radiation, excited by well collimated X-rays, emitting isotropically from the foil had an effective solid angle of 2π against the crystal. The foil could be removed to a distance from the crystal but still in the path of the collimated beam of X-rays, where the solid angle subtended by the sample was negligibly small while the intensity of the exciting beam remained the same. By subtracting the latter spectrum from the former, the intensity of the K X-ray emitted by the sample could be calculated. The initial vacancy produced in the K-shell, was calculated with the help of K photoelectric absorption coefficient, the total absorption coefficient, the absorption jump ratio and the number of photons in the direct beam.

Calibrated Geiger-Muller counters have been used for detecting fluorescent radiation from elements excited following radioactive decay, the energy of the radiation being determined by absorption method (Kinsey, 1948b). The number of initial vacancies was determined by measuring either the α- or the β-disintegration rate.

Several summaries of the magnitude of the K Auger effect have been published. The summaries of Arends (1936) and Backhurst (1936) for example, cover the

contemporary data on fluorescence yields very well but do not include any measurements on the heavy elements. The complete summaries of Burhop (1952) and Broyles et al. (1953) include the collected data on elements of atomic number greater than 56. Recently a new and complete summary has been given by Gray (1955[6]) and Roos (1957) has reviewed the data available for the heaviest elements.

Theoretical: The first attempt to outline a theory of the Auger effect was by Wentzel (1927), who, using a two-electron atom of high nuclear charge, was able to show that the reciprocal of the life-time of a K-shell vacancy, with respect to an Auger transition in which an L electron is emitted, should be independent of Z. Since the reciprocal of the effective life-time of an excited K state with respect to radiation of X-rays is approximately proportional to Z^4, ω_k, the K-shell fluorescence yield, may be expressed by the equation

$$\omega_k = Z^4/(k + Z^4) \quad ,$$

where k is a constant. Such an expression, however, can only be qualitatively correct because any complete and accurate theory of the Auger effect must be based on a proper theory of quantum electrodynamics since the effect involves the interaction of several electrons rather than only two.

Calculations of the fluorescence yield have been made by Burhop (1935) and Pincherle (1935) using a non-relativistic theory and by Massey and Burhop (1936) using a relativistic theory. In these calculations, hydrogen-like single electron wave functions were used, the effective nuclear charge being determined by the application of Slater's rules (1930). The use of screened, hydrogen-like wave functions in the relativistic calculations increases the calculated Auger probability for elements of high atomic number. Relativistic effects are of some importance even for elements of atomic number as low as 47. When allowance is made for screening and relativistic effects the variation with Z of the fluorescence yield is given in the form

$$\left(\frac{\omega}{1-\omega}\right)^{\frac{1}{4}} = A + BZ + CZ^3$$

where the constant A includes the effect of screening and C that of relativity. Burhop (1955) determined the values of the constants A, B and C from a least squares fit of the experimental data on the fluorescence yield of the K-shell. They are given in the table below together with the results of Laberrigue-Frolow and Radvanyi (1956) and Hagedorn and Wapstra (as quoted by Nijgh et al. 1959).

VALUES FOR THE CONSTANTS A, B AND C.

	Burhop	Laberrigue and Radvanyi	Hagedoorn and Wapstra
A	0.004	0.022	0.064
B	0.0346	0.0318	0.0340
C	1.35×10^{-6}	1.14×10^{-6}	1.03×10^{-6}

The experimental values support in a qualitative way the theoretical predictions.

L-Fluorescence Yields:

The experimental information on the L-shell fluorescence yields, on the other hand, is less complete than that for the K-shell.

Direct measurement of the total fluorescence yield of the L-shell has been carried out for 21 elements in the range of Z from 40 to 92 by Lay (1934) using X-rays to excite the fluorescence and photographic film to compare the intensities of the incident and fluorescent radiation. Care has to be exercised in the interpretation of the L fluorescence yield since the relative excitation of the three subshells depends critically on the mode of excitation, and the fluorescence yields for the subshells L_I, L_{II}, L_{III} will in general be different.

Measurements of the fluorescence yields for the individual subshells were made with ionization chambers by Küstner and Arends (1935) for seven elements in the range of Z from 73 to 83, using X-rays with energies lying between the absorption limits of L_{III} and L_{II}, L_{II} and L_{I}, and just above the L_{I} level respectively, interpreting the increase in the yield of secondary radiation at the absorption edges as the characteristic radiation due to the higher level.

There are five possible ways in which vacancies may be produced in the L-shells, viz., fluorescent excitation, internal conversion of γ-rays, reorganization of the atom ionized in the K-shell, electron impact, and by L-capture. For each of these the relative ionization probabilities in the L_{I}, L_{II} and L_{III} subshells are different. Therefore different values of $\bar{\omega}_{L}$ may be obtained depending on the method employed to produce the initial ionization.

Another difficulty in the study of the fluorescence yield of the L subshells arises from the fact that the L-shell vacancy may be shifted from one subshell to another by Coster-Kronig transitions (Coster and Kronig, 1935). This effect is particularly important in the heavy elements where the L_{I} -L_{III} M_{IV}, M_{V} transitions - transfer of ionization from the L_{I} to the L_{III} level with the ejection of an M_{IV} or M_{V} electron - are energetically possible, and where ~~because of the fact that~~ the total width of the

L_{III} level is approximately equal to the total widths of the M_{IV} or M_V levels in the heavy elements.

Taking this effect into account, the fluorescence yields of the L_I and L_{II} subshells, ω_{L_I} and $\omega_{L_{II}}$ such as measured by Küstner and Arends may not be the true values in the region of Z where the Coster-Kronig transitions are energetically possible. The values of $\omega_{L_{III}}$, however, remain unaffected and measurements of $\omega_{L_{III}}$ made by Stephenson (1937) for Pb, Th and U bear this out. His results are consistent with the corresponding measurements of Küstner and Arends which suggests that both sets of measurements for $\omega_{L_{III}}$ are reliable. (see however Chapter VI).

Kinsey (1948a) estimated the values of ω_{L_I}, $\omega_{L_{II}}$ and $\omega_{L_{III}}$ for a few elements in the range of Z from 73 to 92 in an indirect way, by estimating the radiation width of each subshell and dividing this by the total width of the subshell. Estimates of the radiation width were based on the calculations by Massey and Burhop (1936) of the absolute transition probabilities of selected strong radiative transitions, and also on the measured relative intensities of all important lines in the L X-ray spectrum arising in the particular L subshell. For the total widths, Kinsey selected a 'best value' from the direct measurements of level widths made for Ta and W by Bearden and Snyder (1941) and for Au by Richtmyer, Barnes and Ramberg (1934).

The Coster-Kronig yield was calculated by dividing the partial width of the L_I level due to the Coster-Kronig transitions, Γ_C, by the experimental values of the total width of that level. The values of the partial width were given by the measurements of Cooper (1942), and Γ_C was assumed to arise only from ionization transfers of the type $L_I - L_{III} M_{IV,V}$. To check the validity of this method of calculation the values obtained in this way were compared (Kinsey, 1948b) with those obtained by direct measurement of the fluorescence yields of Tl and Bi arising from the internal conversion of Y-rays following the β-disintegration of ThB, the α-disintegration of ThC and the β-disintegration of RaD. He thereby established that his calculated values were rather low and also that the fraction of this yield due to ($L_I + L_{II}$) fluorescence was larger in the cases of ThC and RaD than the calculations predicted. He concluded therefore that some of his initial data were in error and also that Coster-Kronig transitions of the type $L_I - L_{II} N$ occurred in about 12 % of the L_I ionizations.

Ross et al. (1955) have examined critically all the existing experimental data on fluorescence yields of the L levels of Bi excited by internal conversion of the Y-ray from RaD and by soft X-rays. They have developed a set of equations based on Kinsey's (1948a)

assumption that the L fluorescence yield of an atom singly ionized in a given L level is, to a good approximation, the same as the L fluorescence yield for an atom ionized both in the given L level and in an M or higher level.

The more important of the relations are reproduced below.

$$n_1 + n_2 + n_3 = I = A + F \tag{1.1}$$

$$\omega_1 n_1 + \omega_2(n_2 + f_{12}n_1) + \omega_3[n_3 + f_{13}n_1 + f_{23}(n_2 + f_{12}n_1)] = F \tag{1.2}$$

$$a_1 n_1 + a_2(n_2 + f_{12}n_1) + a_3[n_3 + f_{13}n_1 + f_{23}(n_2 + f_{12}n_1)] = A \tag{1.3}$$

$$n_1 = n_2/C_2 = n_3/C_3 \tag{1.4}$$

$$\omega_1 n_1 = \frac{\omega_2(n_2 + f_{12}n_1)}{F_2} = \frac{\omega_3[n_3 + f_{13}n_1 + f_{23}(n_2 + f_{12}n_1)]}{F_3} \tag{1.5}$$

$$a_1 n_1 = \frac{a_2(n_2 + f_{12}n_1)}{A_2} = \frac{a_3[n_3 + f_{13}n_1 + f_{23}(n_2 + f_{12}n_1)]}{A_3} \tag{1.6}$$

$$1 = f_{12} + f_{13} + \omega_1 + a_1 \tag{1.7a}$$

$$1 = f_{23} + \omega_2 + a_2 \tag{1.7b}$$

$$1 = \omega_3 + a_3 \tag{1.7c}$$

where n_1, n_2, n_3: the numbers of primary ionizing events per disintegration in the L_I, L_{II} and L_{III} levels respectively.

ω_1, ω_2, ω_3: the fluorescence yields of the three L levels.

a_1, a_2, a_3: the Auger yields of the three L levels.

$f_{12}f_{13}f_{23}$: the Coster-Kronig transition yields for transfer of ionization from the level represented by the

first suffix to the level represented by the second suffix.

I, F, and A: the total number per disintegration of L ionization, L fluorescent quanta and L Auger electrons respectively.

R : the total number of γ-quanta radiated per disintegration.

$1:C_2:C_3$: the relative numbers of primary ionizations in the three levels.

$1: F_2: F_3$: the relative numbers of L X-ray quanta produced from the three levels.

$1: A_2: A_3$: the relative number of Auger electrons produced from the three levels.

The object of these equations was to find the quantities represented by small letters in terms of those represented by capital letters which were experimentally determined. Since, however, these equations are neither independent nor sufficient an additional source of information was necessary. Lacking this some simplifying assumptions had to be made and the assumption $f_{23} = 0$ was considered the most satisfactory. If however no assumption was made a second set of experiments was required in which the primary ionization was produced in such a way that the ratios of the number of vacancies in the three L subshells were different from $n_1 : n_2 : n_3$. Data concerning the X-ray excitation of Bi obtained by Robinson and Young (1930) and results

from the β-disintegration of RaD were taken in their calculations for the two sets.

However, the accuracy of the information on which their evaluation was based was not always of the same order and in particular the individual values of the Auger yields from the three L subshells were difficult to determine with precision.

Outline of Present Investigation:

Since this study attempts to increase the accuracy of our knowledge of the L fluorescence yields for heavy elements and of radiationless transfers of ionization within the L subshells, an outline of the method used will now be presented.

If the initial vacancies are produced only in the L_{II} and L_{III} shells, the above equations reduce to

$$n_2 + n_3 = I = A + F \qquad (1.1)'$$

$$\omega_2 n_2 + \omega_3(n_3 + f_{23} n_2) = F \qquad (1.2)'$$

$$a_2 n_2 + a_3(n_3 + f_{23} n_2) = A \qquad (1.3)'$$

$$n_2 = \frac{n_3}{C_3} \qquad (1.4)'$$

$$\omega_2 n_2 = \frac{\omega_3(n_3 + f_{23} n_2)}{F_3} \qquad (1.5)'$$

$$a_2 n_2 = \frac{a_3(n_3 + f_{23} n_2)}{A_3} \qquad (1.6)'$$

$$1 = f_{23} + \omega_2 + a_2 \qquad (1.7a)'$$

$$1 = \omega_3 + a_3 \qquad (1.7b)'$$

where C_3, F_3 and A_3 are now the ratios of the numbers of primary ionizations, L X-rays and Auger electrons produced in the two levels, L_{II} and L_{III}.

Omitting from consideration equation (1.3)' and equation (1.6)' since they contain quantities A_3 and A which are difficult to measure accurately, we are left with six equations, five of which contain the quantities ω_2, ω_3, f_{23}, a_2 and a_3 which it is our purpose to determine. Although there are five equations involving these five unknowns together with the experimentally determined quantities I, C_3, F and F_3, nevertheless these equations are not all independent. It is therefore necessary to acquire some further information and for this reason recourse must be had to the published values for one of these five unknown quantities. After a critical examination it has been decided that the figures available for ω_3 are the most accurate and hence these have been accepted. ω_3 having been eliminated from the 'unknown' category, it is now possible to solve the equations explicitly for the remaining four unknown quantities, viz.:

$$\omega_2 = \frac{F}{I}\,\frac{1 + C_3}{1 + F_3} \qquad (1.8)$$

$$f_{23} = \frac{\omega_2}{\omega_3} F_3 - C_3 \qquad (1.9)$$

$$a_2 = 1 - \omega_2 - f_{23} \qquad (1.10)$$

$$a_3 = 1 - \omega_3 \qquad (1.11)$$

According to the Unified Nuclear Model of Bohr (1954), in an even-even nucleus well removed from closed

shells, there exist rotational levels and these rotational levels should decay by cascade E2 transitions to the ground state. The probability of producing ionization in the L_{II} or L_{III} shell is very high following internal conversion of a low energy E2 transition whereas it is very low for the L_I shell.

Cm^{242} is an alpha emitter of 162.5 days half-life with α-energies of 6.110 MeV leading to the ground state of Pu^{238} (73.7%) and 6.066 MeV leading to the first excited state of Pu^{238} (26.3%). (Fig. 1). The 44 keV γ-ray accompanying the de-excitation of the latter state is heavily converted in the L and M shells. This transition, like most transitions from the first excited state to the ground state in even-even nuclei, is of multipole order E2. It has been so characterized by measurements of the total internal conversion coefficients and of the L subshell ratios. Other α-rays of 5.964 (0.035%) and γ-rays of 104 keV (0.006%) and 157 keV (0.0027%) have been reported by Asaro et al. (1953) but their intensities are too small to contribute any effect on the fluorescence yield measurements. Hence in this work account has been taken only of the 44 keV transition.

If the internal conversion coefficient of the γ- ray were known, the fluorescence yield, $\omega_L = F/I$, could be calculated by measuring the absolute intensities of L X-rays and also the total disintegration rate. The Cm^{242} source however contains a certain amount of contaminant, in particular Cm^{243} which also emits α-particles followed

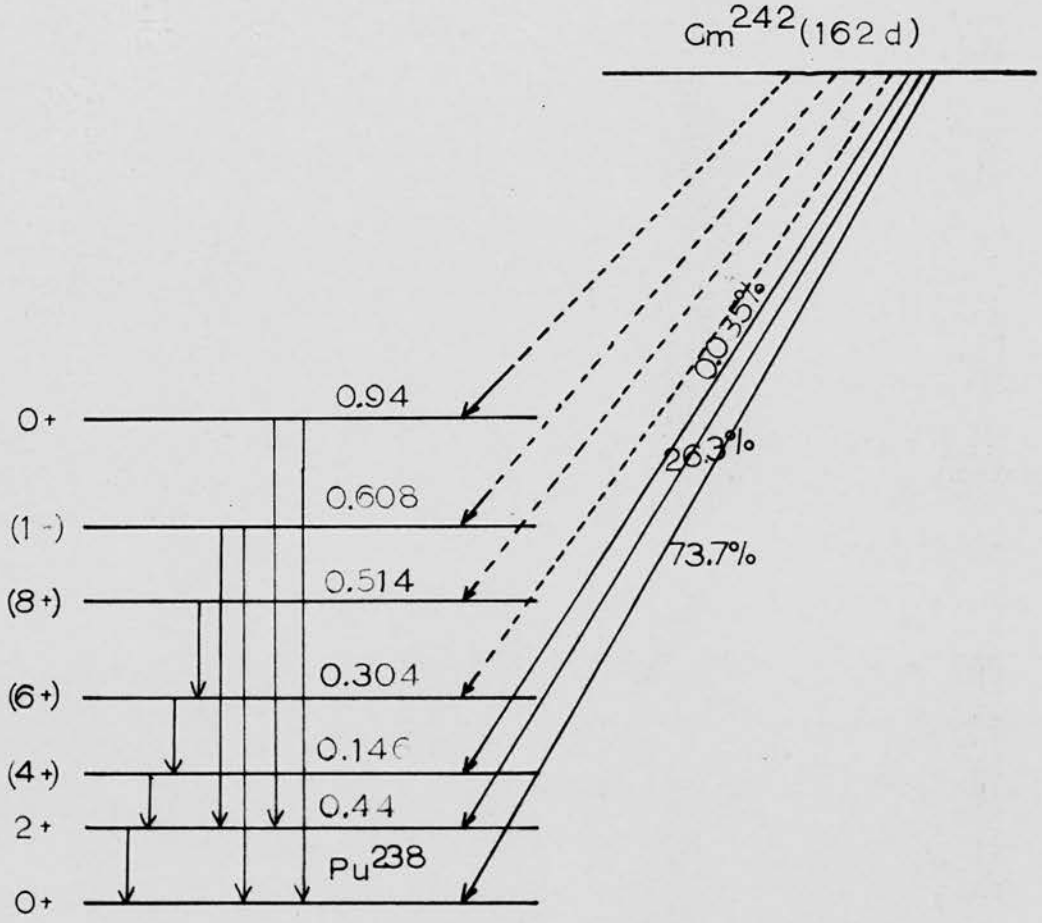

FIG. 1: Cm^{242} Disintegration Scheme.

(Strominger et al, 1958)

by the L X-rays. However the α-particles from Cm^{242} and Cm^{243} are well separated in energy and hence it is possible to eliminate any errors arising from the presence of Cm^{243} by observing only those L X-rays which are in coincidence with α-particles of the correct energy.

A coincidence arrangement has therefore been incorporated into the experiment which consists essentially of a gridded parallel plate ionization chamber to detect the α-particles and a thallium-activated sodium iodide crystal scintillation spectrometer to detect and measure the L X-rays. The relevant theory of the arrangement is set out below.

Let $\Omega_\alpha, \Omega_\gamma$ be the fractional solid angles presented by the source to the α-particle detector and the X-ray detector respectively.

Let $N_{\alpha o}$ be the number of Cm^{242} α-particles recorded per unit time,

$N_{\gamma co}$ be the number of L X-ray photons in coincidence with a Cm^{242} α-particle (i.e. number of Cm^{242} L X-ray photons) recorded per unit time,

N_α be the true number of α-particles emitted per unit time = total number of disintegrations per unit time,

$N_{\gamma c}$ be the true number of Cm^{242} L X-ray photons emitted per unit time.

Then
$$N_\alpha = \frac{N_{\alpha o}}{\Omega_\alpha} \qquad (1.12)$$

and
$$N_{\gamma c} = \frac{N_{\gamma co}}{\Omega_\alpha \Omega_\gamma} \qquad (1.13)$$

so that

$$\frac{N_{\gamma c}}{N_a} = \frac{N_{\gamma co}}{\Omega_a \, \Omega_\gamma} \qquad \frac{\Omega_a}{N_{ao}} = \frac{N_{\gamma co}}{N_{ao}} \quad \frac{1}{\Omega_\gamma} \qquad (1.14)$$

The ratio $\frac{N_{\gamma c}}{N_a}$ leads to a value for F/I when the total internal conversion coefficient in the L shell and the population of the first excited state of Cm^{242} are known, the final result being

$$\frac{F}{I} = \frac{N_{\gamma c}}{N_a} \cdot \frac{N_a}{I}$$

$$= \frac{N_{\gamma co}}{N_{ao} \cdot \Omega_\gamma} \cdot \frac{\alpha(\Sigma) + 1}{0.263 \times \alpha(L)} \qquad (1.15)$$

$\alpha(\Sigma)$ being the Total Internal conversion coefficient, $\alpha(L)$ the L shell Internal conversion coefficient.

CHAPTER II

THE IONIZATION CHAMBER

Introduction

In selecting an instrument for the detection and measurement of α-particles in the type of experiment under discussion there are two prime requisites which must be borne in mind. First of all we must demand that the instrument have sufficient energy resolution to separate out completely the two main alpha particle groups which are present in the source, and secondly, since a coincidence experiment is being performed, a high collecting power must be available.

The highest resolution so far obtained has been that given by magnetic spectrographs (e.g. Pilger, 1957) with full width at half maximum about 0.1 % of the line energy. With this instrument, however, only one alpha particle in about 5000 reached the detector and the source was limited to a very small area. With an ionization chamber a large solid angle for alpha particle detection is provided, a fact which compensates for the considerably poorer resolution which is forthcoming, although in fact the resolution as obtained by Cranshaw et al. (1948) with a gridded ionization chamber -- a full width at half maximum of 50 keV for the 5.30

Mev α-particles from Po^{210} -- would be quite sufficient for our purpose. Taking these facts into consideration together with the advantage that the strength of the source is not critical for ionization chamber measurements, it appears that this instrument is almost ideally suited for use in this experiment and hence it has been selected.

Theory of Operation

When a charged particle traverses a gas, its electric field, on interacting with the orbital electrons of the molecules of the gas, may eject some of them, leaving trains of electrons and positive ions along its track. After travelling a certain distance in the gas the particle may dissipate all its energy in this fashion and the total number of ion pairs thus formed depends on the nature of the gas and the type and energy E of the particle. The ionization chamber principle depends on the fact that these ion pairs may be separated by an external electric field and collected on electrodes, the resulting electrical pulse being accurately proportional to the total number of ion pairs formed provided, of course, that the particle expends all its energy in the sensitive volume of the chamber. Such an instrument has also another property that, if the amount of energy which

the particle loses on the average to form one ion pair (W ev) remains constant over the whole track length of the particle, the electrical pulse may be taken as a direct measure of the particle energy.

A considerable dependence of W for electrons in air was found by Gerbes (1935), his data being represented by

$$W = 31.62 + \frac{5.27}{\sqrt{(E - E_i)}} \text{ eV}$$

E being the initial energy of the electron in keV and E_i the mean ionization potential of air in keV (0.017). For α-particles Gray (1944) has modified the above equation to

$$W = \frac{31.6}{3.6} + \frac{2.6}{\sqrt{(E\alpha - E_i)}} \text{ eV}$$

where E_α is now the initial energy of the α-particles.

Gases other than air reveal a less marked variation of W with E, the rare gases and hydrogen being found to be particularly good in this respect. Cranshaw et al. (1948) have shown that the ionization-energy curve in argon is linear within the experimental error for alpha-particles of energy 5 to 9 Mev.

An ionizing particle always releases electrons leaving heavy positive ions and if the electrons remain free they will be collected in times of the order

of a microsecond or less. On the other hand, if they are captured to form heavy negative ions, their time of collection is about 10,000 times longer (for the operating conditions and the gas mixture adopted in the present work). When captured their probability of disappearance by recombination with positive ions is also greatly increased. Since the fastest possible collection of electrons is necessary in the ionization chamber when a high counting rate, together with good energy resolution is required, as is the case in coincidence experiments, complete elimination of electro-negative gases such as oxygen is essential.

The discrepancy between the times of collection of the positive ions and the electrons raises a complication in the fast parallel plate ionization chamber. Although positive ions are not collected by the anode, they induce electric charge on it, thereby making the pulse height dependent on the track orientation. This can be seen from the following analysis which essentially follows that given by Wilkinson (1950).

Suppose an ion pair is formed at a distance from the anode (Fig. 2) when the potential difference between the plates is V volts. Let the charge induced on the anode due to the electron be q - and that due to the positive ion be q_+ , since at the time of

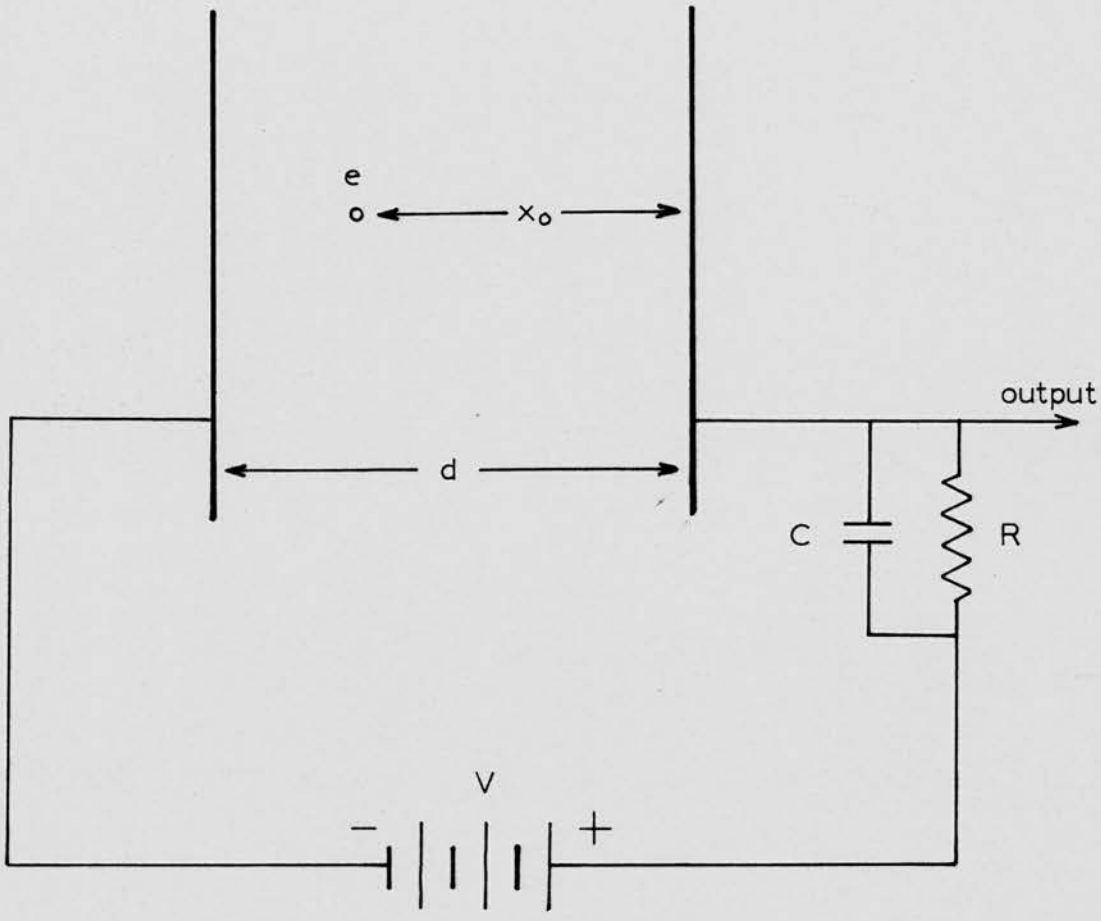

Fig. 2 Fundamental Parallel Plate Ionization Chamber

production the position of both charges is the same, then at t = 0 we have

$$q_-(0) = -q_+(0) = -e\left(1 - \frac{x_0}{d}\right) \qquad (2.1)$$

where d is the distance between the plates. After a time t the electron has drifted a distance vt to a point x, v being the velocity of the electron. We assume that t is so short that the heavy positive ions may be considered as remaining stationary. Therefore

$$q_-(t) = -e\left(1 - \frac{x}{d}\right) \qquad (2.2)$$

and since the potential rise P of an isolated electrode with capacity C on which is placed a charge q, is given by

$$P = \frac{q}{C}$$

Therefore the anode potential change is now

$$P(t) = \frac{q_+(t) + q_-(t)}{C}$$

$$= \frac{e}{C}\left\{-\left(1 - \frac{x}{d}\right) + \left(1 - \frac{x_0}{d}\right)\right\}$$

$$= -\frac{e}{C} \cdot \frac{vt}{d} \qquad (2.3)$$

The pulse therefore rises linearly until $t_1 = x_0/v$, when we have

$$P_1 = -\frac{e}{C}\,\frac{x_0}{d} \qquad (2.4)$$

The scope of the method is widened by the use of a grid in the chamber. This effectively gives the first differentiation directly, and leaves only the second to be performed electronically. Instruments of this nature were made by Alfven (1935) and recently, in more modern form, by Frisch (1944).

Consider a chamber containing a grid of parallel wires of spacing ξ, wire radius r, placed at a distance a from the collecting electrode A and a distance c from the other electrode C (Fig.3). The potentials of the electrodes A and C are V_A and V_C respectively and that of the grid is V_G. We now consider our ion pair to be formed at ℓ, a distance b from the plane of the grid. The charge induced by the positive ion on A will no longer be $-e(c - b)/(a + c)$ as in the no-grid case considered above, since some of its lines of force finish on the grid instead of on A. Thus the collecting electrode is in some measure protected from the positive-ion effects which rendered a simple parallel-plate chamber useless for accurate energy analysis. The electron proceeds to A and gives its full pulse as before (assuming that it is not collected by the grid, an effect discussed below).

The degree of shielding afforded by such a grid has been calculated by Buneman et al. (1949). It is

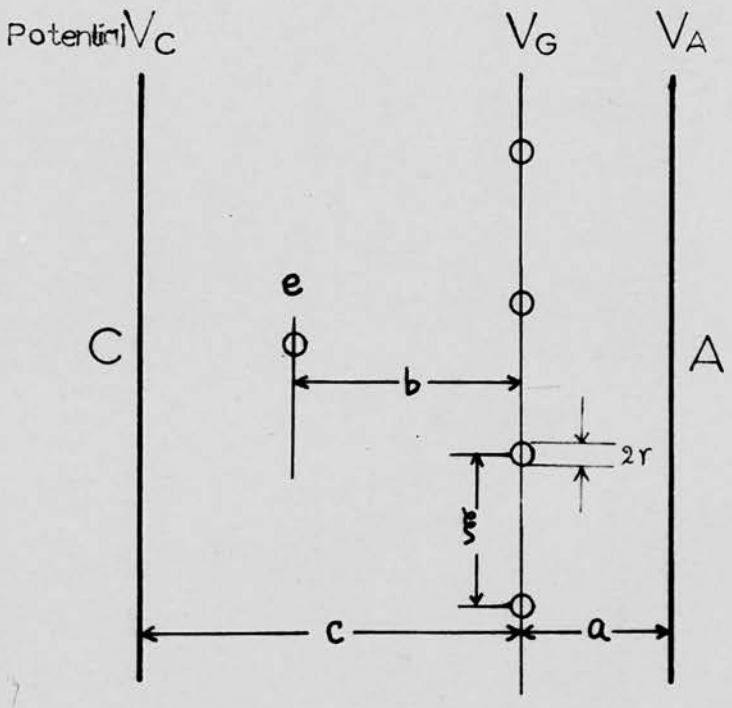

FIG. 3: Gridded Ionization Chamber.

expressed in terms of a parameter $\sigma = \frac{dE_P}{dE_Q}$ where E_P is the field strength between the grid and anode, E_Q is that between the positive ions and the grid. σ is a function of the grid constants r/ξ and ξ/c, and is called the inefficiency of the grid. The charge induced by the positive ion at x_0 on the anode is given by

$$Q_+ = e\sigma\left(1 - \frac{b}{c}\right)$$

The expression for σ is complicated, but in the desired limit of small σ may be written, for not too large $2\pi r/\xi$

$$\sigma \approx \frac{\xi}{2\pi a} \log \frac{\xi}{2\pi r} \qquad (2.5)$$

If the ionization can be formed reasonably far from the grid this method allows pulses of very uniform height to be obtained from randomly oriented tracks.

The remaining important question in connection with gridded chambers concerns λ, the fraction of the electrons collected on to the grid, instead of on to the anode, and so lost so far as pulse production is concerned. If λ were constant the only objection to such a loss would be the reduction of pulse size, but λ cannot be accurately constant as its value will depend somewhat on the orientation of the ionization path if this is formed at all close to the grid.

Such an effect introduces an additional variance in the pulse-size distribution. One should therefore be assured of the smallness of λ. Buneman et al. (1949) have exhibited a relationship between $1 - \lambda$ and $\frac{V_A - V_G}{V_G - V_C} \frac{c}{a}$ both theoretically and experimentally, for a few values of $2\pi r/\xi$, $\frac{V_A - V_G}{V_G - V_C} \frac{c}{a}$ being the ratio of the field strength between the grid and the anode to that in the body of the chamber. Finally, it might be mentioned that the presence of a grid produces an additional benefit in that the rise time of the pulse is improved.

Design and Construction.

The ionization chamber was made from a horizontal cylinder of brass about 15 cm. in diameter and 18.7 cm. long, closed at both ends by means of screws and rubber rings and normally filled with argon gas (90%) and methane (10%) to a pressure of one atmosphere. It was connected to the gas purifier by a brass tube of 2 cm. diameter. Both the vacuum system and the filling system were brass cylinders of large diameter and vacuum (black out) was always reached within a few minutes. The grid was placed at an adjustable distance of 7.5 to 8.5 cm. from the cathode and a potential of 540 volts was applied to it. A brass ring carrying a voltage intermediate between this potential and

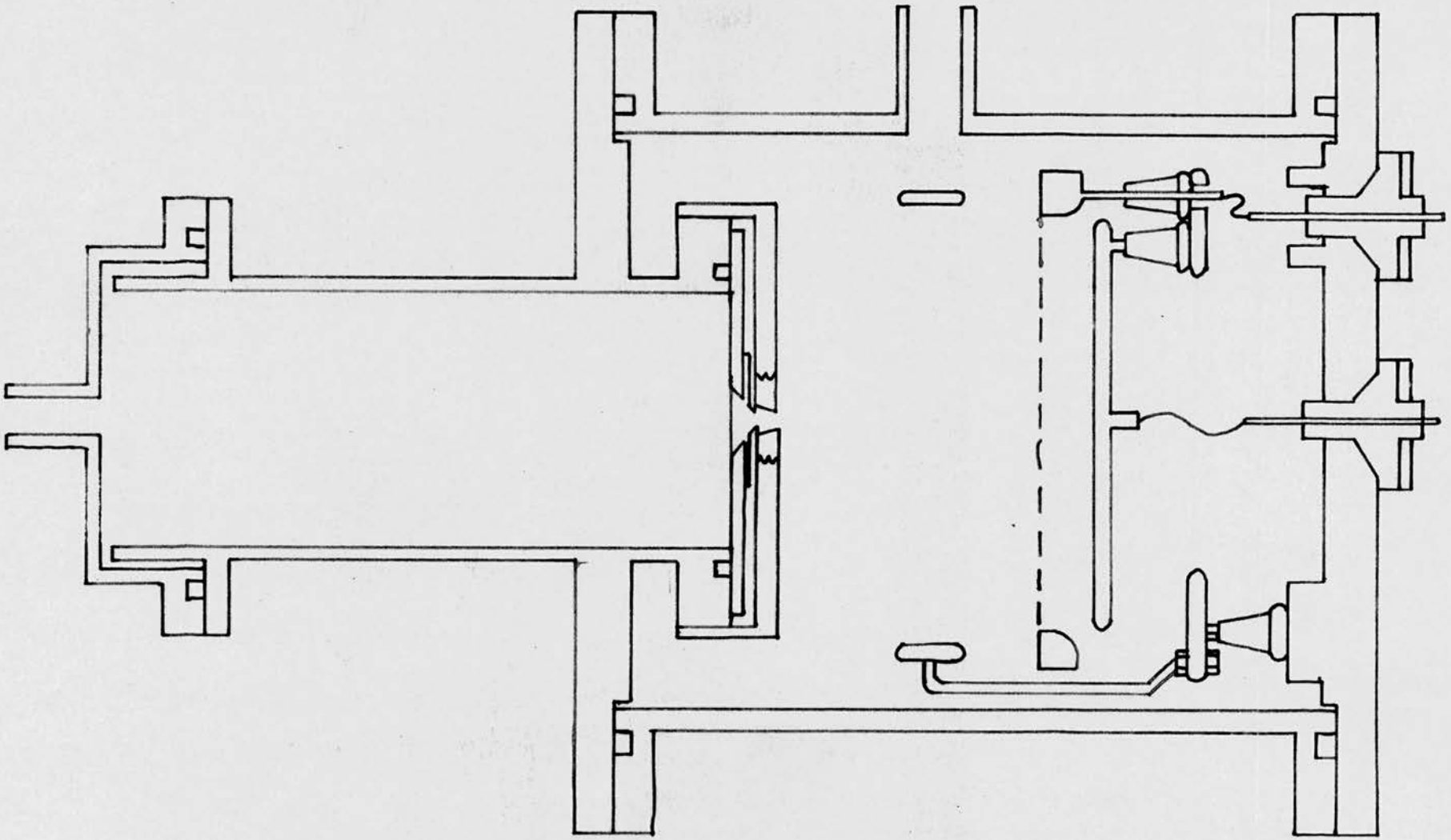

FIG. 4: The Ionization Chamber in Plan.

earth was placed between the grid and the source holder to provide a more uniform electric field. A collecting electrode consisting of a brass disc, 10 cm. in diameter and with the edges rounded off and polished to prevent any discharge, was placed 9.2 cm. from the source holder and was designed as small as possible to keep its electrical capacity at a minimum.

Insulators for the leads to each electrode were made from polythene and were shaped as shown in the Fig. 4. At the high voltages used the glass-to-metal seal originally present did not withstand the H.T. and was often the cause of electrical noise in the output.

In designing the grid two main factors were considered (i), grid inefficiency, (ii) collection of electrons by the grid.

In the present study two grids were made. The first one consisted of a brass ring of 12 cm. diameter having parallel wires of 0.23 mm. diameter with a 1 mm. spacing between them. One end of each wire was soldered to the brass ring which had parallel grooves of 1 mm. spacing in it and the other end was araldited and set. Soldering both ends would give rise to a slackening of tension in the wires when the grid was cooled and even the grid made in this manner had lost its tension after a few months. Moreover the wires were

hardly kept parallel. When the grid was placed 1.8 cm. from the collector its inefficiency was calculated to be ~~0.00125~~ 0.0029. Electron collection of the grid depends largely on the ratio of the grid-anode field to the grid-cathode field and also on the ratio $2\pi r/\xi$ (Fig. 3).

Due to the mechanical difficulties in the first grid a second grid was made on a stouter brass ring with copper wires of 0.33 mm. diameter and spacing 1.52 mm. In grid no. 2 σ was kept nearly the same as in grid no. 1 and the electron collection was kept as low as possible by increasing the field ratio. For this purpose the grid-anode distance was decreased as far as possible (to the extent just not to affect σ seriously) and a higher voltage of 1460 volts was applied between the anode and the grid, while the grid cathode potential difference was kept at 540 volts.

When these voltages and the grid-anode distance were well adjusted to minimize the electron collection by the grid, the energy resolution was as good as with grid No. 1. No difficulty has been experienced by the rather high field ratio. However, the writer feels that it would be safer to lower this ratio by using finer wires than those used in grid No. 2, copper wire being replaced by tungsten wire, and anchoring them through fine holes drilled on the ring.

To minimize the energy loss suffered by the α-particles it was preferable to place the source inside the chamber, thus eliminating any need for a window. On the other hand, when the chamber was used in coincidence experiments it was necessary to provide a window for photons. The active material was therefore deposited on a thin aluminium foil of 0.68 mg/cm^2 and it was confined within a circle of 3 mm. Over the source was placed an aluminium foil of thickness 6 mm., having a hole 3 mm. in diameter in it, the hole being concentric with the source, since an α-particle collimator was necessary to remove the most oblique tracks, and thus to improve the ratio of wanted to unwanted counts. Although it is possible to use a larger shallower hole to improve the geometry, while still retaining resolution by choosing suitable time constants in the differentiation and integration circuits of the amplifying system (Bertolini et al., 1954), oblique tracks were undesirable in coincidence experiments for the following reasons: (1) It is important that the rise time of the pulses should be well correlated in time with the passage of the ionizing particle. (ii) Oblique tracks suffer more energy loss in the source itself, thus increasing the width of the pulse height spectrum. The difference between the times of collection of electrons from most oblique tracks and

of those from tracks normal to the source backing was calculated from the experimental information on electron drift velocities in the gas mixture given by English and Hanna (1953) and is approximately 0.5 μsec. The coincidence resolving time would have to be increased by this amount if a higher geometry collimator were used.

The source holding disk was mounted on a brass cylinder as shown in Figs. 5 and 6 and the entire block was made to slide into position for the easy handling of the source. In order to protect the source backing from the pressure difference while sliding in, large holes (six holes of ¼ inch diameter each) were provided at the sides of the cylinder and wide and deep slots underneath the source holder to enable the air to escape. ~~(see Figs. 5a and b).~~

In order that the L X-rays should pass through with minimum absorption loss, a thin window constructed from a light element was required. This is particularly important when uncertainties are involved in the spectral composition of the L X-rays. In its original form this window was made from aluminium foil 0.05 mm. thick, the absorption loss for Cm^{242} L X-rays introduced by this window together with the source backing and the protective covering over the sodium iodide

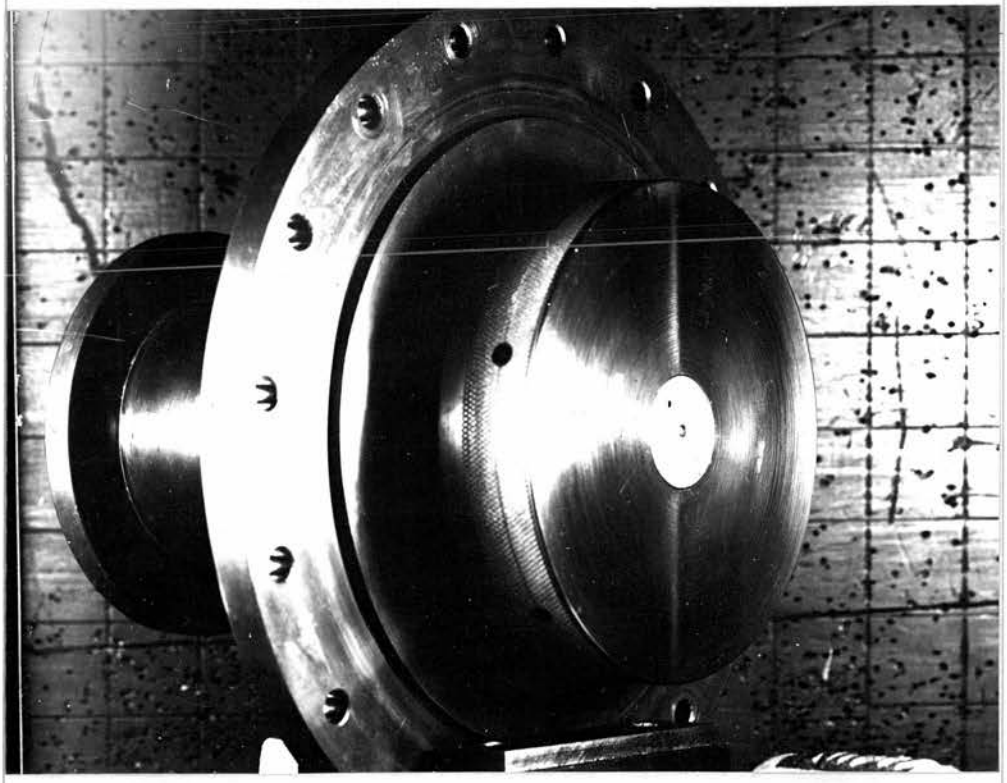

FIGURE 5a

The Source Holder (Front View).

FIGURE 6b

The Source Holder (Rear View)

crystal, being about 15 per cent, however this was later replaced by a thin polythene sheet of superficial density 3.1 mg/cm^2. The absorption loss in this case was about 6 per cent. It should be noted that the source always had to be arranged facing the ionization chamber rather than the scintillation counter. Owing to the use of a thin window the chamber was operated at a pressure of one atmosphere having this disadvantage over higher operating pressures that the positive ion effect on the anode was increased. To protect this thin window against the pressure difference while evacuating and filling, a cap was provided at the end of the brass tube, both sides of the window being evacuated slowly through a needle valve. After the chamber was filled with the gas, the cap was removed and the scintillation counter slid in through the tube (Fig. 7).

In selecting a grid-to-cathode distance there are several considerations which must be kept in view. The range of a 6.110 Mev α-particle in argon at atmospheric pressure is about 5 cm. (Livingston and Bethe, 1937) and hence the grid-to-cathode distance must be at least 5 cm. In any case, longer distances favour reduced positive ion effect and reduced electron loss at the grid. These advantages are counter-balanced to some extent by the fact that the electron collection

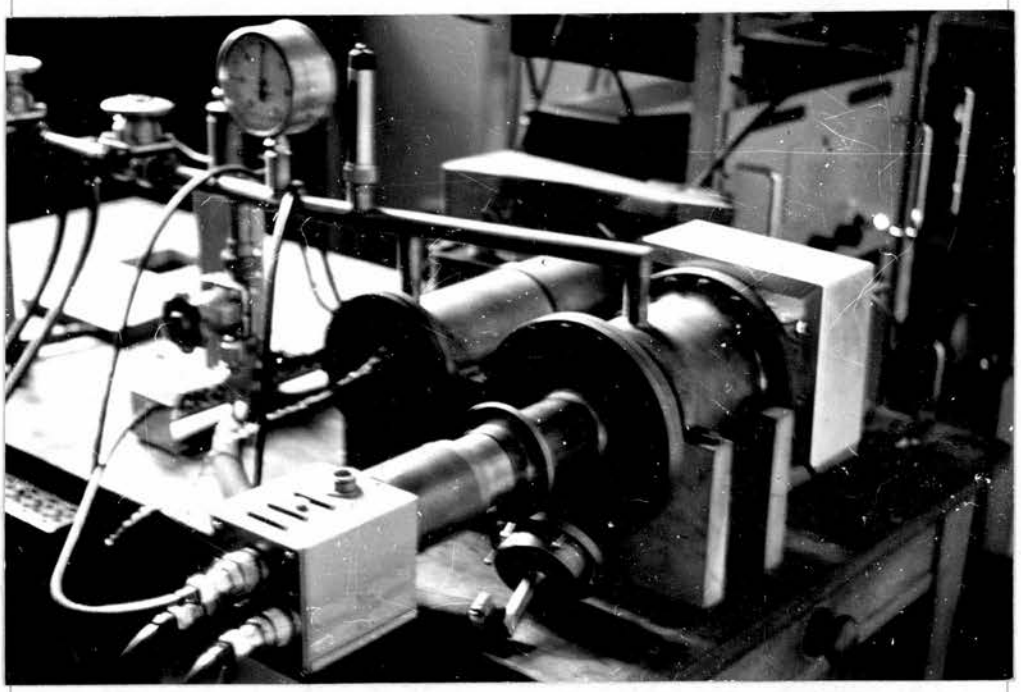

FIGURE 7

Ionization Chamber and the Scintillation Counter

time also increases under these conditions. In selecting a grid-to-cathode distance of 8.5 cm. it is felt that a proper balance has been maintained between these conflicting factors.

In order to keep the chamber gas free of oxygen a purifier was attached and the argon kept circulating by convection. This purifier consisted of a brass cylinder 29 cm. long and 10 cm. in diameter closed at either end by vacuum-tight plates, containing a porcelain tube filled with calcium turnings. This tube was heated by D.C. current through a 100 Ω nickel resistor and kept at a temperature of 350°C as measured by a thermo-couple. To reduce heat loss to the surroundings by radiation an aluminium reflector tube, ~~concentric~~ coaxial with the porcelain tube, was also incorporated in the device. This purifier proved very satisfactory and when it was kept running constantly over a few weeks, the change in pulse height observed was less than 0.6 per cent.

Operation of Chamber

The lowest electrical field strength in the space between the grid and the source holder is determined by the electron velocity needed to give a short rise time to the pulse and the required degree of saturation in that region, where the saturation is defined as the

field strength that will prevent recombination of electrons and positive ions.

This electric field strength is determined as follows. A relatively high voltage of 1800 volts is required between the grid and the anode and since the source is normally at earth potential and both the grid and the anode are well above earth potential, a power unit of floating type is most convenient for supplying a constant voltage between the two electrodes. A power unit of this type was not available so in practice a power unit supplying 1800 volts was connected between the anode and the grid, the grid being kept at earth potential, and another was connected between the grid and the cathode, the cathode being kept negative with respect to earth potential. The pulse height was constantly watched while the potential of the second power unit was varied and a constant pulse height was reached at about 500 volts. Above this voltage no appreciable increase in pulse height was noticed.

The ratio between the grid-to-anode field and the grid-to-cathode field, $\frac{V_A - V_G}{V_G - V_C} \frac{c}{a}$, was determined in a similar manner, the grid-to-cathode field strength being kept constant for this experiment and the anode-to-grid field strength varied. The E.H.T. connection for this purpose is shown in Fig. 8b. The best energy resolution was obtained when the anode-to-

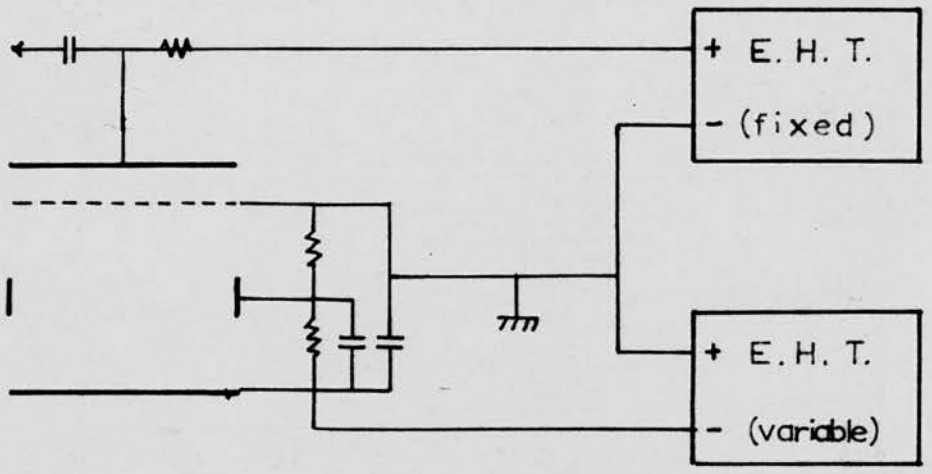

FIG. 8a: E.H.T. Connection for Determination of Grid-to-Cathode Voltage.

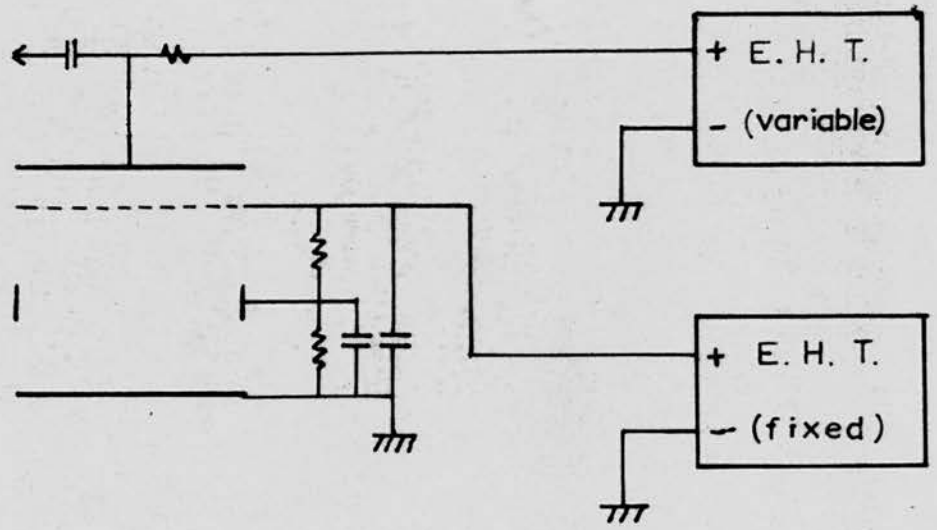

FIG. 8b: E.H.T. connection for determination of

$$\frac{VA - VG}{VG - VC} : \frac{c}{a}$$

cathode potential difference was above 1350 volts, hence the voltage ratio of 1350/500 was chosen. After a voltage divider of this ratio was connected the voltage plateau had a slope of about 0.2 per cent per 100 volts over the range of 1700 volts to 3000 volts and the operating voltage chosen was 2000 volts.

Since it is a well known fact that methane is an excellent "moderating gas" in argon and the experimental results obtained by English (1953) provide good information on argon-methane mixtures, no thorough investigation was made of the effect of varying the gas content of the chamber. However, a preliminary experiment on the variation of pulse height with the percentage of methane in the mixture showed (Fig. 9) that the pulse height is more than doubled in a proper mixture than in pure argon. The pulse height rises steeply with the methane content up to about 1%, after which it rises gradually to its maximum. In the range of 3% to 12% methane addition no significant variation in the pulse height was observed.

Electronics

The electronic arrangement for the α-particle pulse amplifying system is shown in Fig. 10. The E.H.T. was taken from a power unit type 200 capable

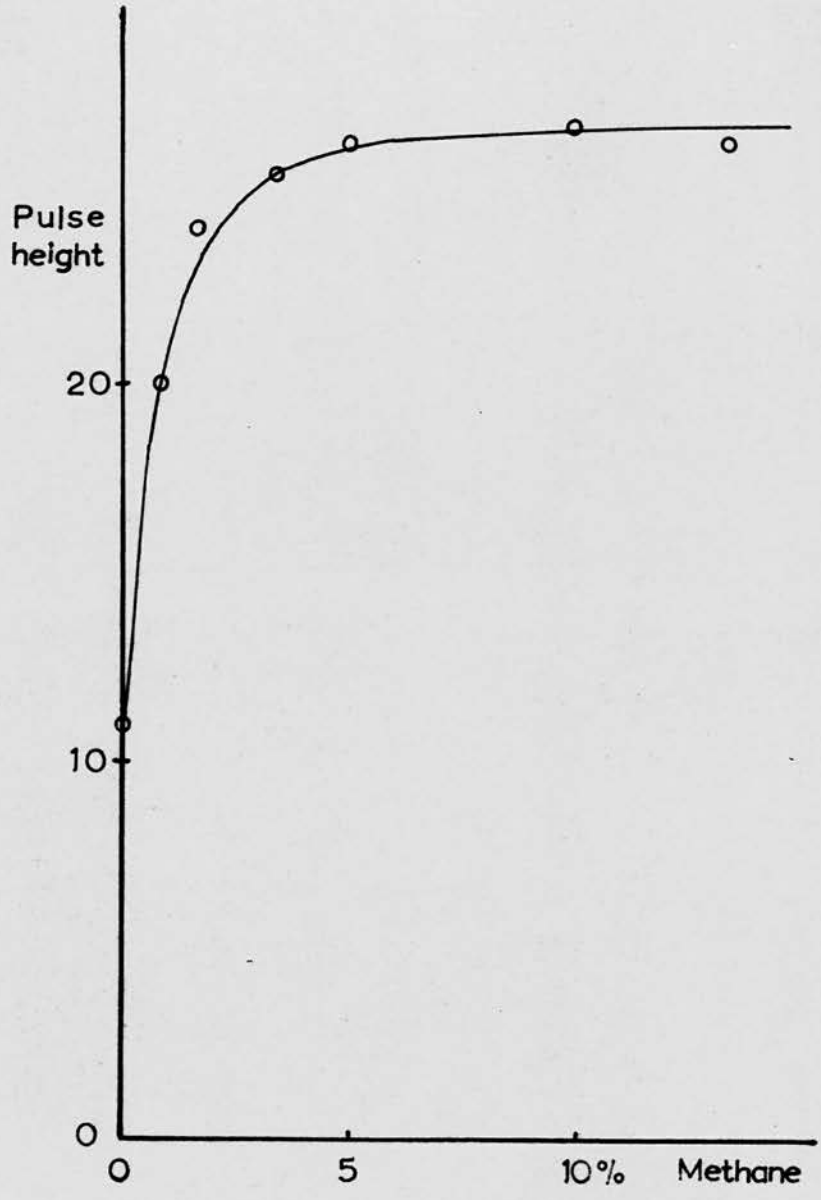

FIG. 9: Variation of Pulse Height with Methane Proportions

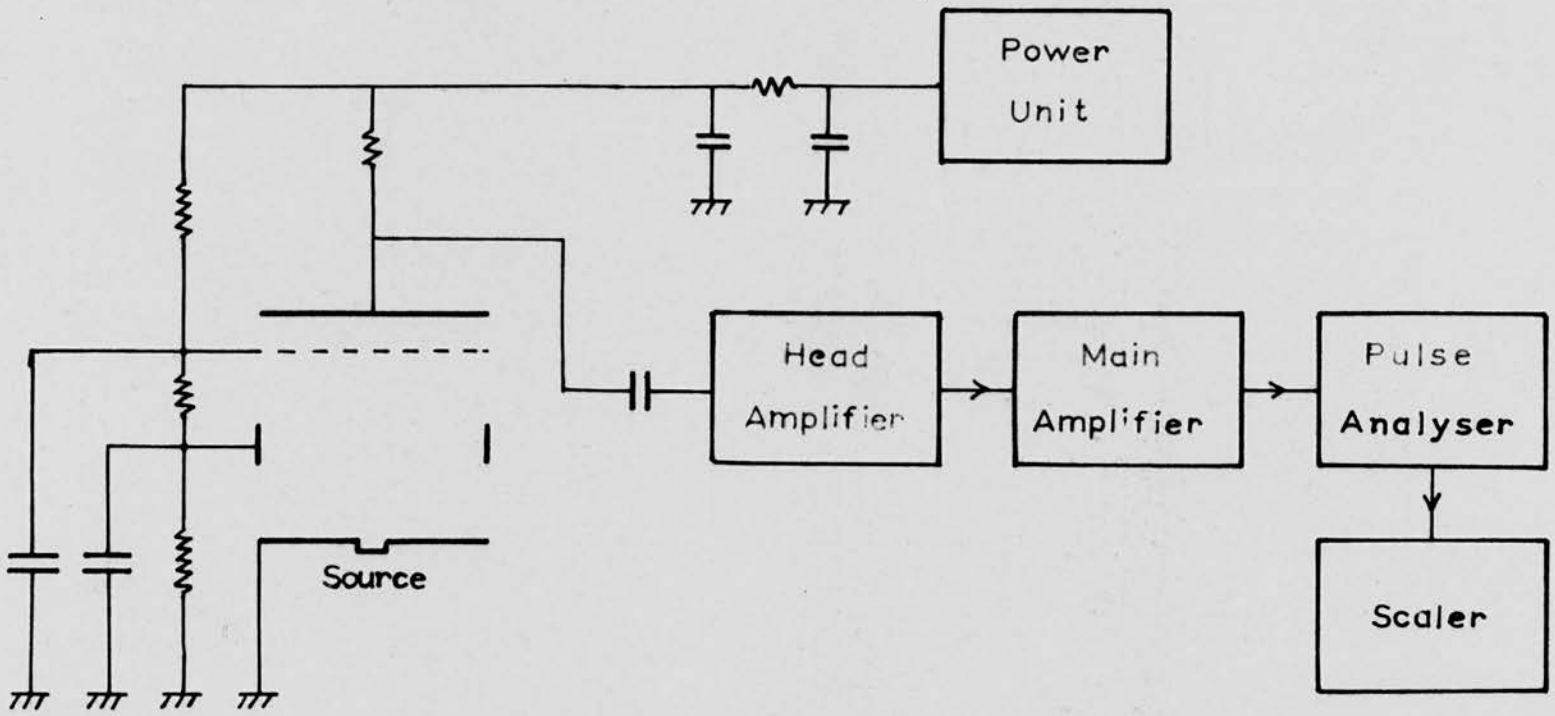

FIG. 10: Electronic Arrangement of α-particle Detector

of supplying a stabilized voltage up to 4000 volts, through an RC coupled filter circuit which reduces to a very low level any hum or spurious pulses which may be present in the E.H.T. All the electrodes including the brass ring between the grid and the cathode were decoupled by means of large 0.5 μF capacitors. The load for the counter was 100 MΩ and the signal from the anode was coupled to the first grid of the head amplifier through a 50 $\mu\mu$F capacitor being amplified 50 or 100 times before transmission to the main amplifier. The main amplifier was a linear amplifier type ECKO N568 and provided variable gain from 46 to 86 db.

The output from this amplifier was fed to a Sunvic Multi-channel pulse height analyser of the Huchinson-Scarrot type where an adequate (usually 36 volts) voltage was subtracted from each pulse, the remaining pulse being amplified further by ten times before analysis. A scalar of Type 200 was connected to the pulse height analyser, taking the integrated counts accepted by it and from this integrated count a correction for the dead time of the analyser could be made.

In the study of energy spectra of α-particles by means of an ionization chamber of this type, it is necessary to reduce to a minimum the broadening of the

spectral lines due to the noise of the first stage of the electronic amplification. Contini et al. (1956) made an extensive survey of valves for use in the minimum noise head amplifier required for fast ionization chambers and have selected for the first input stage the valve E83F as their first choice. This valve was chosen for its very low grid current. A similar head amplifier was constructed for the present study selecting the best of the four E83F valves available. The input stage was a cascade of two triode-connected E83F valves followed by an EF 91 pentode amplifier stage and an EF 91 output cathode. follower. A resistive feed back was carried from the output to the cathode of the first E83F. The loop gain was about 3000 while the feed back stabilized the voltage gain to 100 (Fig. 11).

An alternative head amplifier of type ECKO N568 was acquired with the main amplifier and although the noise level was about 20% higher with the latter it had a better stability and measurements requiring a long period were usually taken with this head amplifier. Some further points in connection with noise in the amplifier will be discussed later when the energy resolution of the ionization chamber is considered.

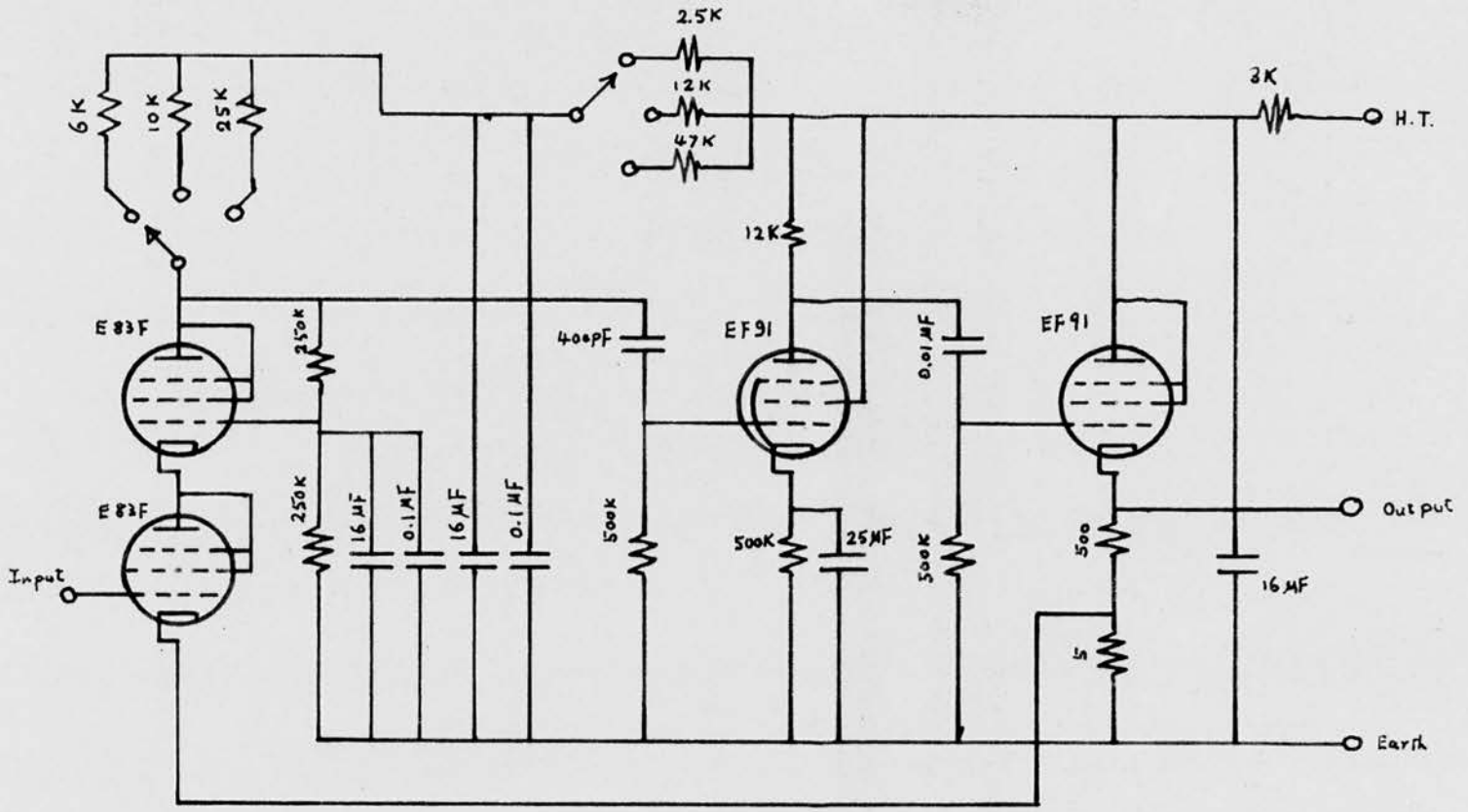

FIG. 11: Circuit Diagram of Low-Noise Head Amplifier.

Noise Level and Energy Resolution.

The energy resolution obtained from any measurement device is affected by the electrical noise in the amplifying system and hence it is always essential to keep the noise level at a minimum. In this work, an upper limit of about 2,500 volts was permissible for the E.H.T. since above this voltage the coupling condenser started to produce excessive noise. There were, it appeared, three methods whereby this effect could be countered. The first of these methods ~~consisted~~ was ~~of using a guard ring~~ to keep the anode at earth potential and the cathode negative ~~cathode~~, since in these circumstances the quality of the condenser is not of major importance when it is a question of noise production. This method has been used by Frisch, and Cranshaw (1948) but could not be used in this work since it was necessary that the scintillation counter also incorporated had to be at earth potential. The other two methods both depended on some means of keeping the operating voltage as low as possible and these will now be considered in turn.

If a collimator of non-conducting material were used the electric field in the collimating hole would be roughly the same as the grid to cathode field provided always that the dielectric constant ε of the material used was close to unity. Under these conditions the field strength near the collimating hole

would be stronger than would be the case for a collimator of conducting material and hence a somewhat lower high tension could be used. Such a method would be ideal if it were only a question of measuring the α-particle energy, since small pulses caused by α-particles scattered at the wall of the collimator, could easily be discriminated against by use of a pulse height analyser. This method was tried but was eventually discarded since the source was so strong that the number of pulses was far too large to be tolerated.

The other method consists of covering the collimating hole with a grid of equally spaced fine wires in order to make the field strength effectively zero within the collimating hole and uniform at the surface of the source holder. This eliminates all uncertainties due to the presence of a field within the collimating hole, though it reduces the resolution somewhat due to the fact that the hole subtends a finite solid angle so that some of the ionization is not collected and this ionization loss is not the same for all tracks. In this work, however, the reduction in resolution was tolerable since it was a small effect, as the track length of any α-particle within the hole was only a very small fraction of its total track length. The method was therefore used, the average track length lost in the hole being only about one-eighth of the shortest track and so the two peaks

in the spectrum due to Cm^{242} and Cm^{243} + Cm^{244} were still easily separable.

One of the several α-particle spectra of Cm^{242} source is shown in Fig. 12 and it is seen that the peaks due to Cm^{242}, Cm^{243} + Cm^{244} and the daughter product Pu^{238} are clearly resolved from each other. The two main α-particle groups of Cm^{242} which are of 44 keV apart are not resolved, a fact which is in agreement with expectations for the present type of detector. The weighted mean energy values are given for the Cm^{242} and Pu^{238} peaks, while the Cm^{243} Cm^{244} impurity peak is discussed elsewhere. Energy calibration by using standard sources was not attempted in this particular case as the chamber construction was slightly modified for the coincidence measurement and calibration was no longer possible under these working conditions. The energy resolution of the chamber is difficult to judge from this spectrum because the α-particle source does not give a single line spectrum and of the three peaks, the Cm^{242} peak has the simplest composition. It is composed of three lines at 6.110 Mev (73.7%), 6.066 Mev (26.3%) and 5.965 Mev (0.035%). Neglecting the contributions of the 5.965 Mev Cm^{242} line and of the high energy α-particles of Cm^{243} which also lie in the same region.

the standard deviation of the Cm^{242} peak was

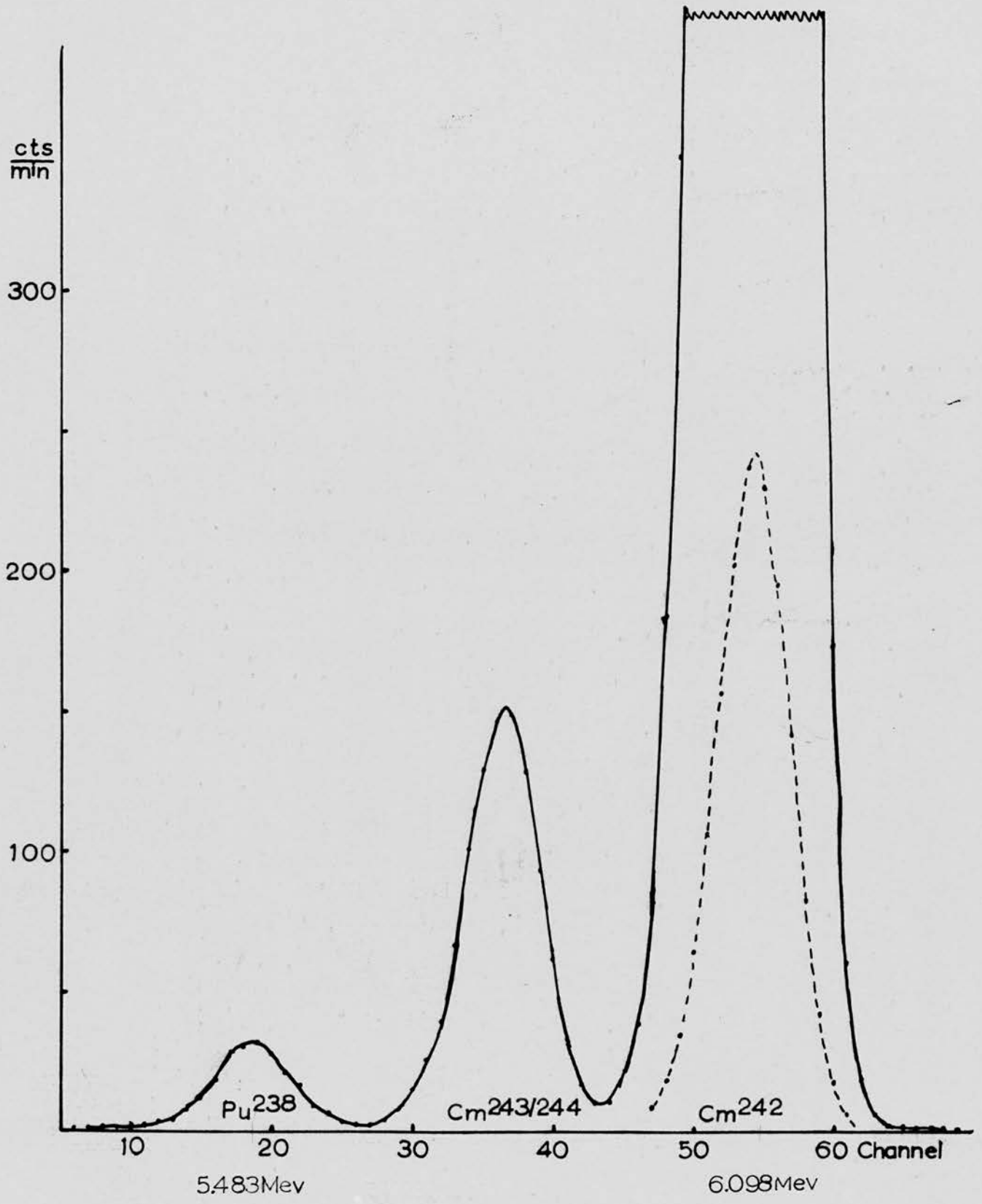

FIG. 12: α-particle Energy Spectrum.

calculated from the original data and if we assume that the two α-particle lines of which this peak is composed are separately of gaussian form, we have the relation

$$N\ \sigma_o^2 = N_1(\sigma_x^2 + d_1^2) \quad N_2(\sigma_x^2 + d_2^2)$$

where

σ_o = measured standard deviation of Cm^{242} peak.

σ_x = standard deviation of either of the two constituent groups.

$\frac{N_1}{N}$ = fractional intensity of 6.066 MeV α group = .263.

$\frac{N_2}{N}$ = fractional intensity of 6.110 MeV α group = .737

$d_1 = |M_1 - M|$, $d_2 = |M_2 - M|$

where M_1 M_2 M are the mean energies of the separate groups and the composite group respectively where $|M_1 - M_2| = 44$ keV.

The variance σ_x^2 of a single α-particle line may be considered as the sum of separate variances due to the following factors:
(1) Energy loss in the source, (2) ionization straggling, (3) Ionization loss in the collimating hole, (4) variation of rise time of electron pulses, (5) induction effect of positive ions, and (6) Amplifier noise. Since they are all independent we may write

$$\sigma_x^2 = \sum_{i=1}^{6} \sigma_i^2$$

Of the separate variances the first five give rise to effects

due to the chamber which are extremely difficult to measure separately and hence we will group them altogether under one variance σ_c^2 so that we may write

$$\sigma_o^2 = \sigma_c^2 + \sigma_n^2$$

where σ_n^2 is the variance arising from the amplifier noise. This was independently determined by feeding uniform pulses from a signal generator attenuated to be the same height as the Cm^{242} α-particle pulses into the amplifying system. The complete experimental results are tabulated below:

TABLE II.1

Standard Deviation in Pulse Height Distribution

	σ_o	σ_x	σ_c	σ_n
Expt. (1)	47.7	43.6	38.7	20.2 keV
Expt. (2)	49.4	45.5	40.6	20.4 keV

Both σ_c and σ_n are larger than those obtained by Buneman et al. (1949) and why this is so is not very clear though the following possibilities suggest themselves. (1) The main factor having an effect on σ_c in the present experiment which was not present in the work of Buneman is that denoted by (3) above, i.e. ionization loss in the collimating hole and it may be that this effect has somewhat greater consequences than

were expected. (ii) For the coincidence experiment it was necessary to have a very sharply rising pulse and hence a short 1.6 μsec. integration time constant was necessary. This increases the anode current noise, thus increasing σ_n though the optimum signal to noise ratio was obtained by having both time constants the same.

CHAPTER III

α-Y COINCIDENCE ARRANGEMENT

Introduction

For accurate measurement of the detection efficiency of the α-particle detector and elimination of the back-ground and source impurity effect on the photon detector, the coincidence arrangement was necessary.

The effective solid angle for the coincidence measurement is the product of the solid angles of each detector and if this is too small the time taken to achieve the necessary statistical accuracy may be impractically long, to counterbalance which the source strength must be raised. This introduces more energy loss of the radiation in the source, and the ratio of random coincidences to the true coincidences depends mainly on the source strength and the resolving time of the coincidence unit. The maximum usable source disintegration rate N is given by the relation

$$\frac{N_C}{N_R} = \frac{\varepsilon'(\Omega_1, \Omega_2)}{2\tau\varepsilon N}$$

where N_C/N_R is the ratio of the true coincidence rate to the random coincidence rate, τ is the resolving time, i.e. the duration of one of the coincident pulses when they are equal, $\varepsilon'(\Omega_1, \Omega_2)$ is the fraction of

pulses in the portion of the spectrum accepted by one analyser that is related by coincidence to the radiation accepted by the other analyser and εN is the fraction of the total number of disintegrations which can be detected by the other analyser. In a particular coincidence set-up, the random coincidence rate is roughly proportional to the square of the source strength, for it is given by $2N_1N_2$ (see Chapter IV for more detailed discussion) - N_1 and N_2 being the counting rates of α-particle and photon counters respectively - while the coincidence counting rate is proportional to the source strength.

Scintillation Counter: The most suitable phosphor for the detection of γ-rays is thallium activated sodium iodide, the iodine atoms being responsible for the high absorption efficiency for γ-rays. The combination of energy proportionality, high efficiency and short pulse duration makes the scintillation detector ideally suited to coincidence spectrometry.

γ-rays, in general, interact with the phosphor by three principal processes: Compton scattering, photoelectric effect, and pair production. In the photoelectric process the γ-ray energy appears as the kinetic energy of a photoelectron leaving only X-rays from the residual atom. In the detection of photons of the energy

investigated in the present experiment, these X-rays are mostly reabsorbed, their energy being very low, and below the K-excitation energy of Iodine. Pair production does not occur at low energy. The Compton process transfers some of the incident γ-ray energy to an electron leaving the remainder as a scattered photon, sometimes of energy almost as great as the original photon. This scattered photon may escape from the phosphor or may be further absorbed.

The thallium activator shifts the photon emission band to 4100 A, which is in the region of maximum spectral sensitivity of the photomultiplier. The decay time of the crystal at room temperature is 0.25 μs.

Sodium iodide is hygroscopic and the crystal is therefore sealed in an aluminium can, and is coated with MgO to reduce light losses at the walls. The NaI(Tl) crystal used in the present work was in the form of a 2 cm. cube. The aluminium can was a specially prepared one for low energy photon detection, the thickness of the window being 5 mg/cm^2 aluminium foil.

The crystal was joined to a photomultiplier tube by silicone grease in order to minimize loss of light quanta and the whole unit including the voltage divider for each electrode of the photomultiplier was enclosed in a brass light-tight housing, with a cathode follower attached at the end of the brass housing.

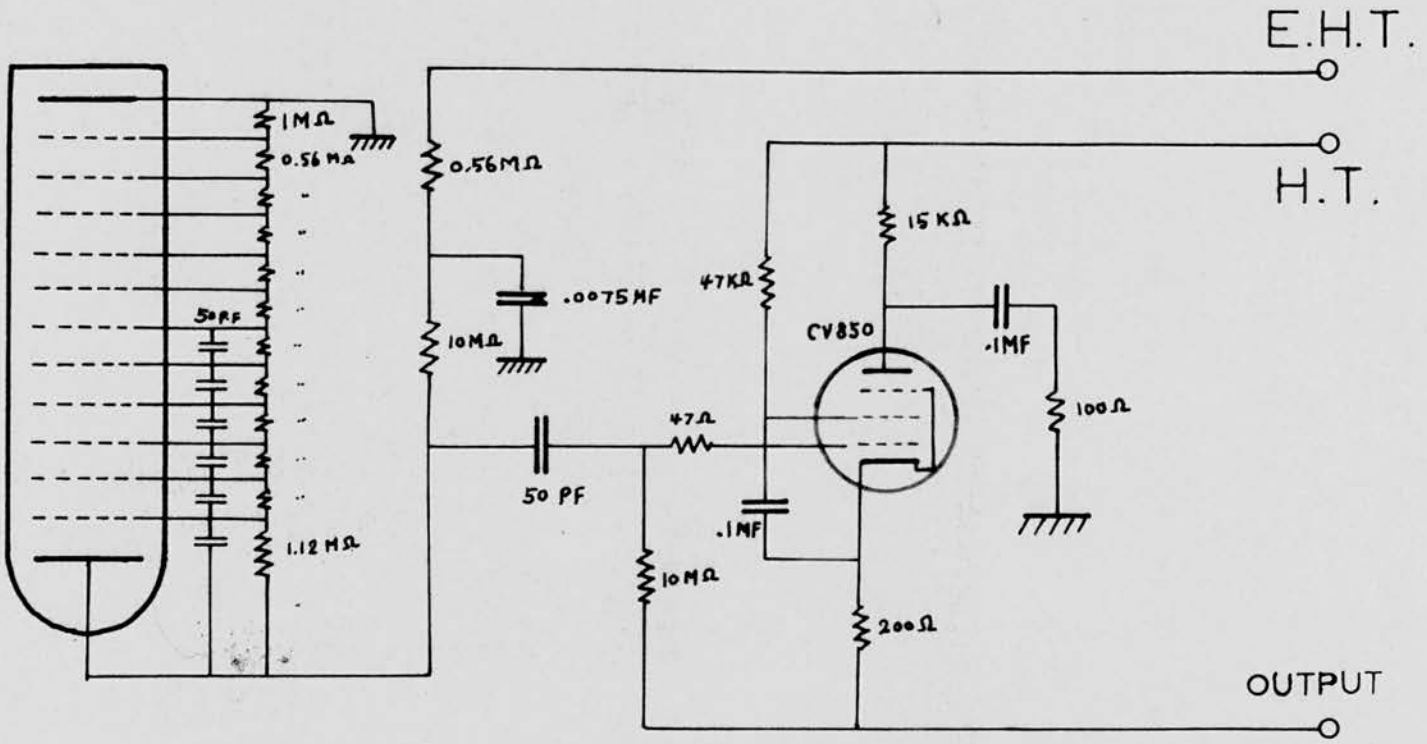

FIG. 13: Photomultiplier and Cathode Follower.

The photomultiplier was an eleven stage EMI 6097 tube and the associated circuit is shown in Fig. 13. The E.H.T. voltage was supplied by a Type 1033A radio-frequency high voltage unit of high stability to the resistance chain with a total anode-to-cathode voltage of about 1350 volts, the anode being positive with respect to earth. This was to ensure that by keeping the cathode at earth potential, there would be no trace of leak current between the photo-cathode and the glass envelope. A higher voltage was applied between the photocathode and the first dynode and between the last dynode and the collector. The former reduces statistical fluctuations in the current pulse while the latter ensures that space charge limitation does not affect the linearity of the multiplier. The decoupling condensers across the last six dynodes ensure that there is no electrical feedback to earlier stages from the large current pulse in the output stages. The differentiating time constant of the photomultiplier output circuit was about a half millisecond, which is about a thousand times that of the phosphor decay constant. When the time constant was shorter (approximately 25μs.) it gave an effect of double differentiation, causing a large overshoot in the output, which was found to be unfavourable to the multichannel pulse height analyser. Therefore a long time constant was found essential for this experiment

the remaining part of the overshoot being rectified by the use of a D.C. Restorer.

One further measure was taken to reduce the effect of edge penetration especially due to the cubed shape of the crystal. A lead collimator with a circular hole of 1.6 cm. diameter was placed in front of the crystal. This provided a well defined window as well as reducing the effect of edge penetration.

The spectrum of photons from the Cm^{242} source, taken with this scintillation spectrometer, is shown in Fig. 14. The energy of the photons was calibrated by using Ir^{192} γ-rays of 295, 308 and 316 keV as an upper energy standard and either the 59.7 keV γ-ray from the disintegration of Am^{241}, or the Cu K X-ray of 7.8 keV excited by Am^{241} γ-rays as a lower energy standard.

The two photon peaks at 226 keV and 278 keV in the spectrum are the γ-rays from the Cm^{243} impurity and the peak in the 104 keV region is also largely of the same origin. The 104 keV line of Cm^{242} is probably too weak to contribute appreciably to this spectrum. A smaller peak at about 80 keV may be partly due to the escape peak of 104 keV photons and partly due to the K X-rays excited in the lead ring used as a collimator. Since no single line photons of suitable energy were available a measurement of the resolution of the spectrometer was not made.

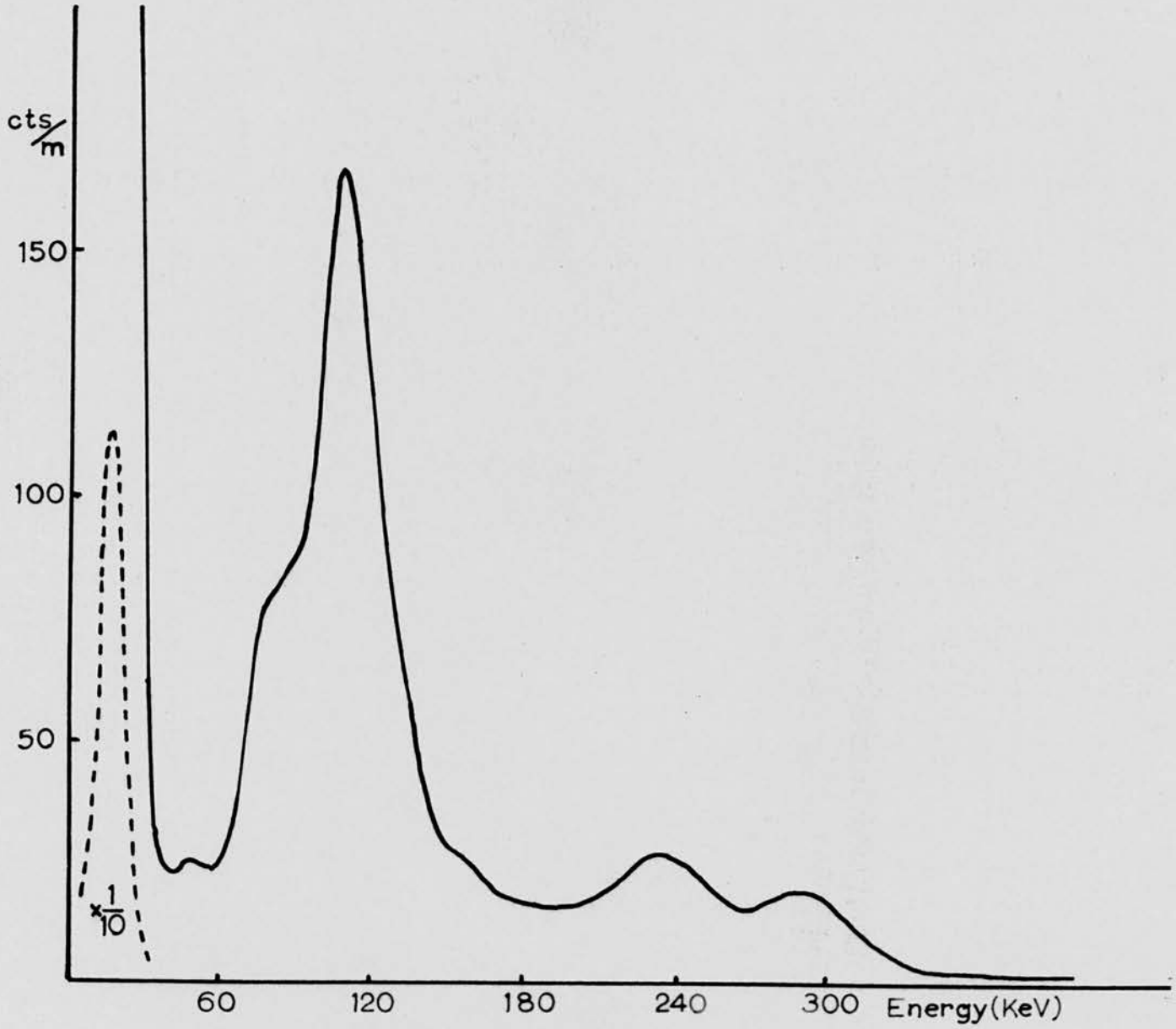

FIG. 14: Photon Spectrum.

Electronic Arrangement: A block diagram of the α-Υ coincidence arrangement is shown in Fig. 15, together with the ideal pulse shape at each stage.

The differentiating and integrating time constants were set at 1.6 μsec. in both main amplifiers and a gating pulse generator combined with a single channel pulse height analyser was put into the ionization chamber circuit when selection of a certain range of α-particle was desired, a subject which is discussed later in more detail. A scaler was connected at the output of the gating pulse generator to measure the α-disintegration rate which is also needed for the random coincidence effect estimation.

Between the cathode follower of the photomultiplier and its main amplifier was connected a delay line to compensate for the time lag between the time of disintegration and the time of collection of electrons at the anode of the α-particle ionization chamber. The Υ-counting rate was taken by a scaler connected at the 'external scaler' output of the multichannel pulse height analyser which could count either the coincidence rate or the photon emission rate of the energy region under investigation. The ~~the~~ photon count was taken before and after each coincidence experiment. The 'external scaler' output circuit of the multi-channel pulse height analyser was such that only pulses that are

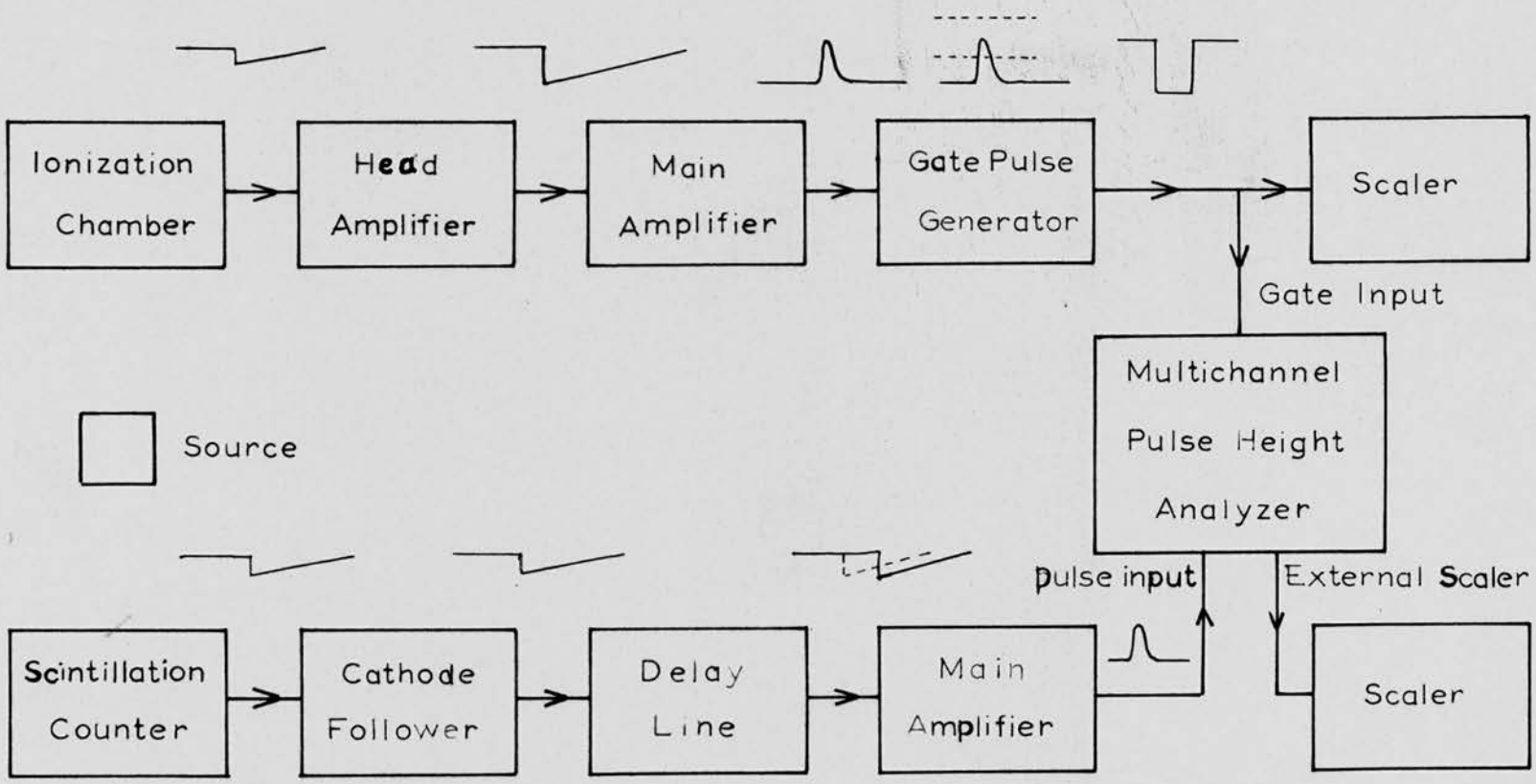

FIG. 15: Block Diagram of Coincidence Arrangement.

sorted by the analyser were counted and not the pulses missed by the pulse height analyser due to its relatively long (741 μsec. average) dead time. This dead time, δ , was calculated by simultaneously feeding random pulses from a radioactive source to the analyser and a separate scaler of known paralysis time (5 μsec.) and then using the formula

$$N = \frac{N_0}{1 - N_0\delta}$$

where N is the true number of pulses arriving per unit time and N_0 is the number of pulses per unit time accepted by the analyser.

The energy region of the photons in the arrangement shown in Fig. 15 was selected by adjusting the bias voltage (0 - 50 volts) and the amplification factor (×1, ×2, ×5 and ×10) provided in the multi-channel pulse height analyser. First, the lower level of the spectrum was set at the required voltage, amplification being set at (x 1). Then the amplification was increased until the desired upper limit was at the highest channel of the analyser. When an adjustment finer than the amplification provided by the analyser was needed, the attennuator provided in the main amplifier (in steps of 2 db.) was employed, readjusting both the lower and the upper limit as before. Although an even finer

adjustment still could be obtained by varying the E.H.T. voltage of the photo-multiplier tube this was not favoured in view of (1) the difficulty in reproduction of the operational conditions, and (2) the change in the characteristics of the pulse shape, which would necessitate readjustment of the delay line and remeasurement of the coincidence resolving time. In any case the energy resolution is not very high in NaI scintillation spectrometers, nor was high resolution necessary. Hence the E.H.T. was set at a constant voltage of 3000 volts most of the time.

Single Channel Pulse Height Analyser: In order to select α-particles in a certain energy band a single channel pulse height analyser was necessary before the pulses were fed into the gating circuit of the multichannel pulse height analyser. This single channel pulse analyser had to be of such a kind that the time lag between the input pulse and the output pulse be constant and not dependent on the pulse height. Such a single channel analyser was not available and hence a special a special one which incorporated a simple germanium diode discriminator had to be constructed for the purpose. The circuit is a combination of a discriminator developed by Park (1956) and a phase inverter and cathode follower to produce negative

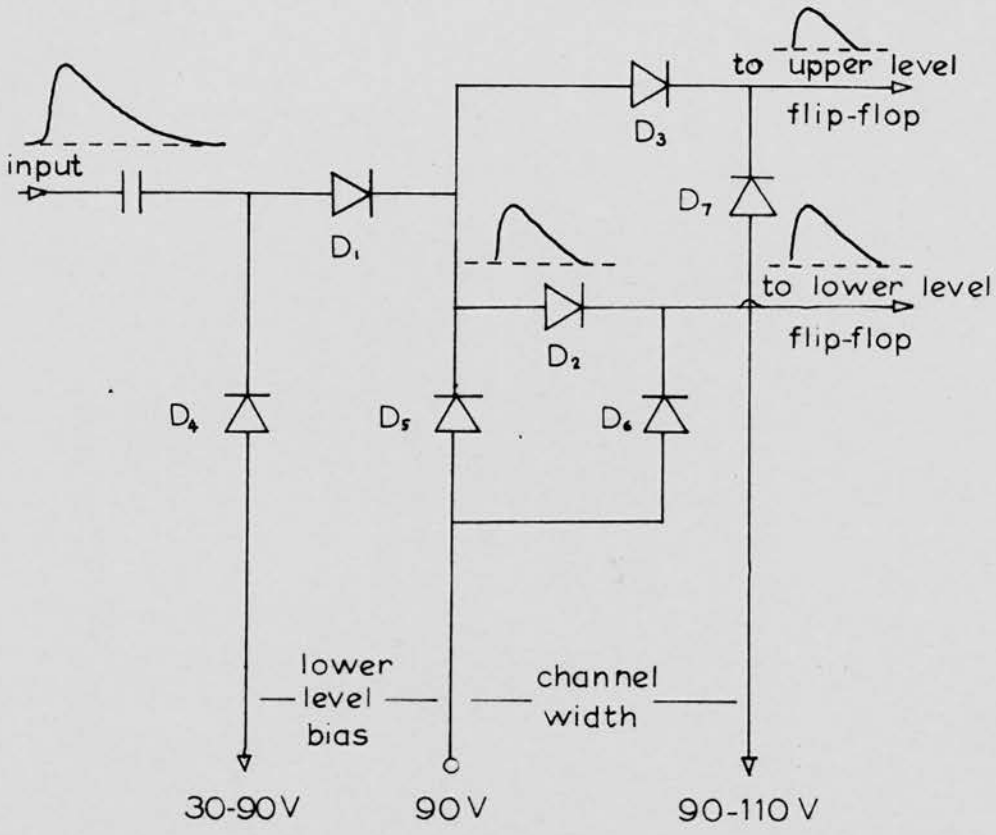

Arrangement of germanium diodes in the discriminator circuit

Figure 16

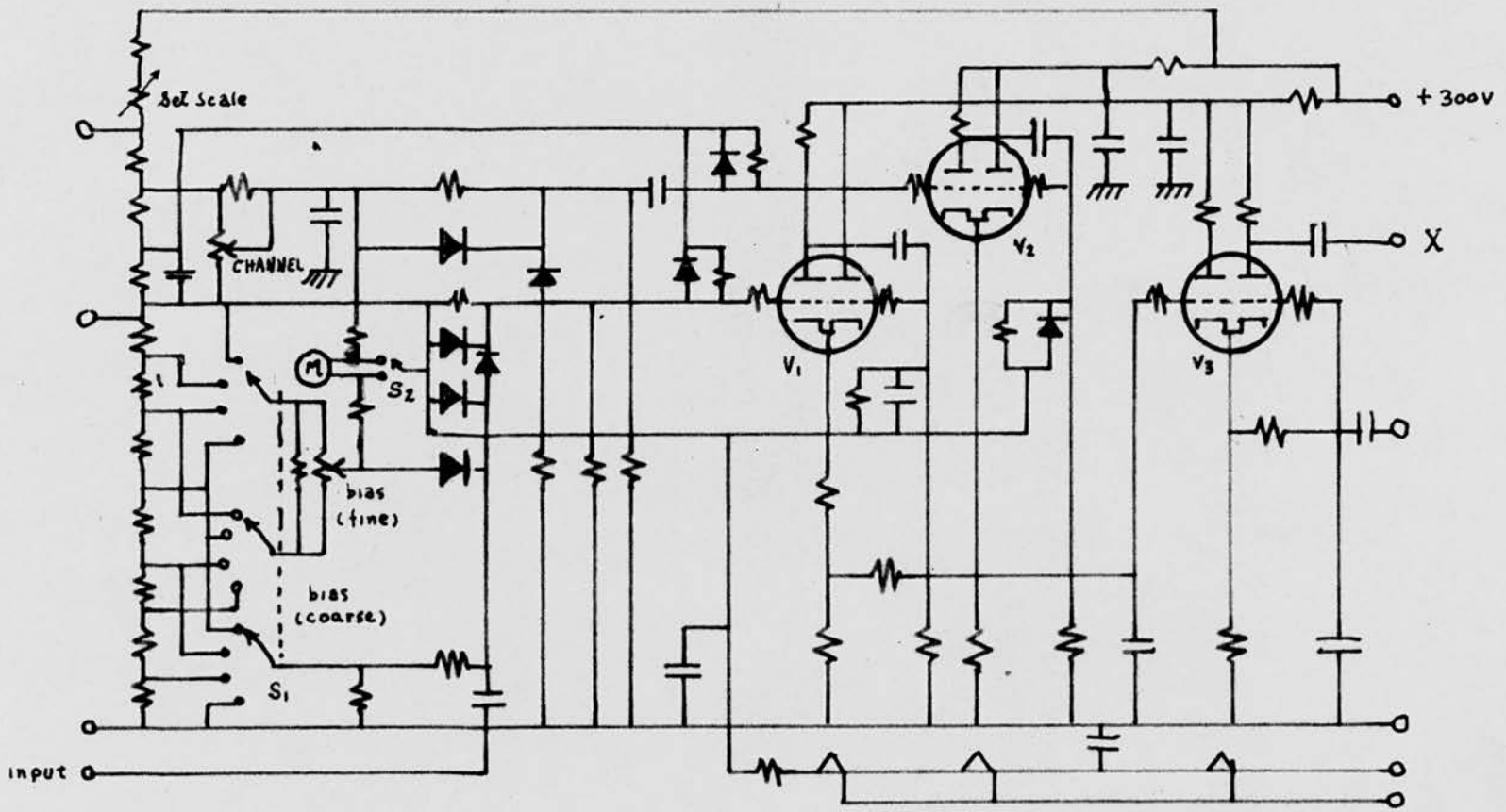

FIG. 17: (Part 1) Circuit Diagram of Gate Pulse Generator.

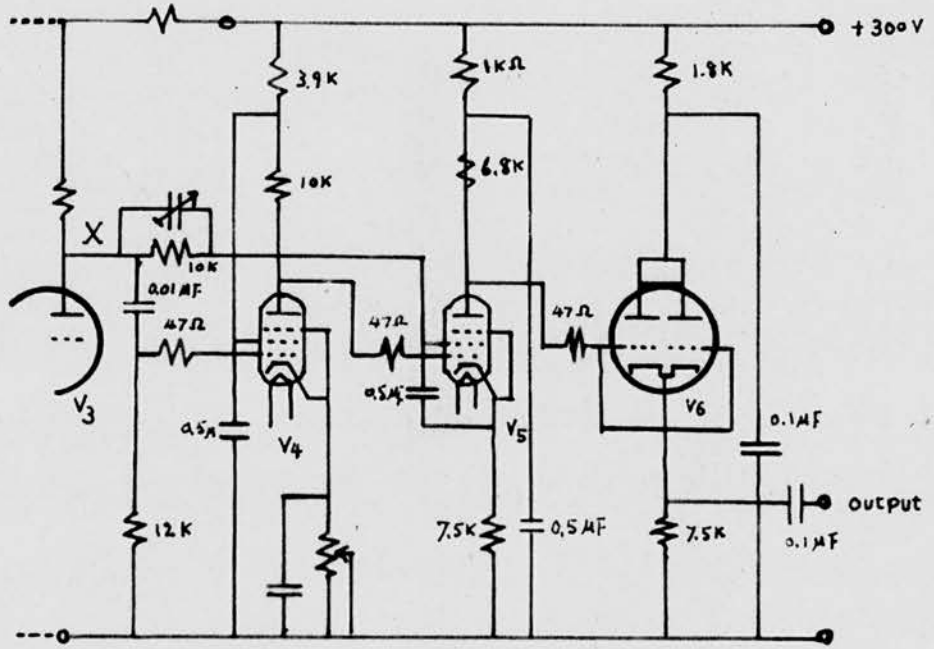

FIG. 17: (Part 2) Circuit Diagram of Gate Pulse Generator.

pulses of about 25 volts required for the gating circuit of the multi-channel pulse height analyser. The discriminator is of the biased diode type and the basic discriminating circuit, arranged to accept positive pulses, is shown in Fig. 16 and the complete circuit diagram is shown in Fig. 17. The lower level of the discriminator can be varied from 0 to 60 volts and the channel width from 0 to 20 volts. Both bias voltages are read directly on a micro-ammeter calibrated from zero to 200 μamp. The first valve is a double diode trigger circuit, determining the lower limit of the discriminator and the second is essentially the same circuit as V_1 determining the upper limit, the length of the trigger pulses of both units being determined by the time constants of the anode-grid coupling circuits (about 1 μsec.) The third double triode V_3 is an anti-coincidence arrangement rejecting pulses exceeding both levels, thus triggering both levels V_1 and V_2, and accepting those pulses that exceed the lower limit bias voltage but not the upper limit. These flip-flop circuits are so designed that they are triggered at, or immediately after, the peak of the pulse and hence the time lags are independent of the input pulse height. All the components used for these three valves are the same as those given in Park's (1956) paper. The theory of operation is given in the same paper and will not be

reproduced here. V4 and V5 together, invert the positive pulses to negative pulses and the combination is followed by a cathode follower V6. Negative feedback is applied via a resistor and a capacitor between V5 and the anode of V3. The V4 cathode resistor is made variable so that the V4 anode potential and the operating conditions of V5 may be set correctly. The output pulse height was set to about 30 volts and the width was about 1.2 μs. at 10% height and 0.8 μs. at 90% height. The output pulse was not strictly a square pulse but its leading and trailing edges were steep enough to keep the coincidence resolving time short.

The analyser was constructed on a V type chassis with the micro-ammeter mounted on the front panel. This type of chassis was very spacious and the components which could interfere with each other were easily separated by placing them on opposite sides. The lower level bias could be set by means of a four position switch (coarse control) and a potentiometer (fine control). The channel width was varied by means of a potentiometer. A switch connected in the ammeter circuit enabled it to be used to read the lower level bias or the channel width as required. The full scale deflection was nominally equal to a bias of 60V or a channel width of 20 V, but calibration was necessary in practice.

Electrostatic screening was provided for all the valves, and the discriminator diodes being grouped together on a tag board were separated as much as possible from the rest of the circuit in order to minimize the effect of temperature variations.

Difficulties were experienced due to spurious pulses being induced in the upper level flip-flop originating in the output circuit and in the lower level flip-flop.

After all the adjustments had been made and the instrument was functioning correctly, it was necessary to calibrate it and in order to do this the following procedure was adopted. The pulses from a pulse generator type 1913C were fed to the amplifier which was set in its normal operating condition (as an α-particle amplifier), to simulate pulses similar to α-particle pulses. The output pulses from the amplifier were fed into the single channel pulse analyser and simultaneously into the multi-channel pulse analyser, calibration being obtained by use of the calibrating test pulses available from the latter.

First, the 'channel height' was calibrated. Before commencing the 'set scale' potentiometer (see Fig. 17) on the analyser was adjusted so that a full-scale reading on the meter was obtained with switch S_2 at 'set bias'. This provided a reproducible voltage

distribution on the potentiometer. Calibrated pulses were now injected and the lower level bias was gradually reduced from its highest voltage to the point at which counting at the output started. A graph of ammeter reading in scale divisions against bias voltage was plotted. This was a straight line with a fixed threshold at zero meter reading (Fig. 18) and provided a calibration curve for the instrument.

The channel width was now calibrated in the following manner. The "Channel Width" potentiometer was adjusted to give a known reading on the meter. Using a fixed pulse height (below 60 volts) from the same pulse generator and amplified as above, the lower level bias was reduced starting from the full reading on the meter until it just started counting. The lower level bias was then equal to the pulse height. This bias was now reduced further until counting in the channel was again stopped, this time because the pulse height was greater than the upper bias level. The difference between the lower level biases in the first and second case was then equal to the channel width, the lower level calibration curve being used. The channel width was altered and the above repeated. A graph of meter reading in scale divisions and channel width in volts was then plotted (Fig. 19), which was a straight line. A small variation in channel width occurred when the lower level bias was

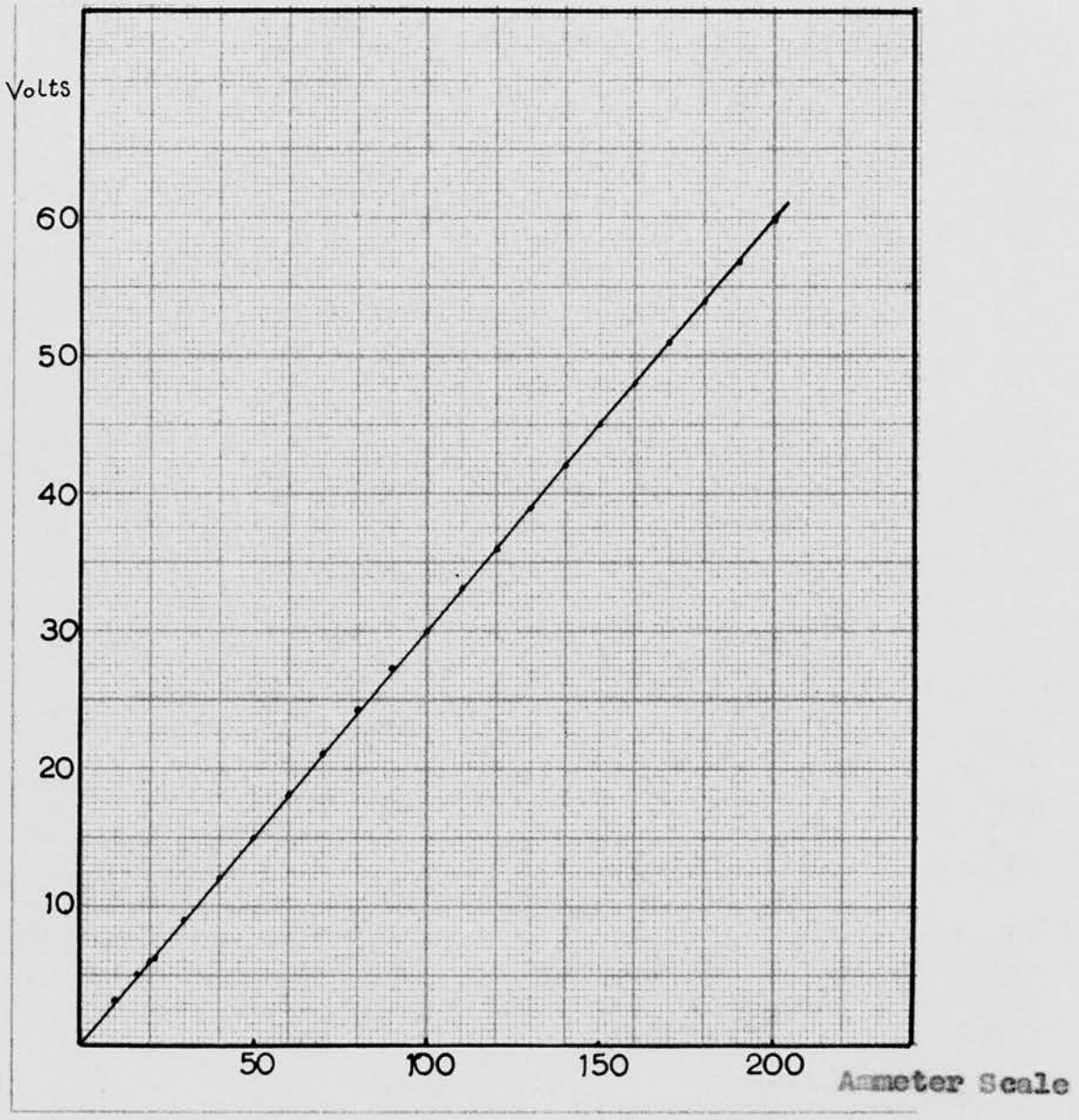

FIG. 18: Bias Voltage Calibration Curve.

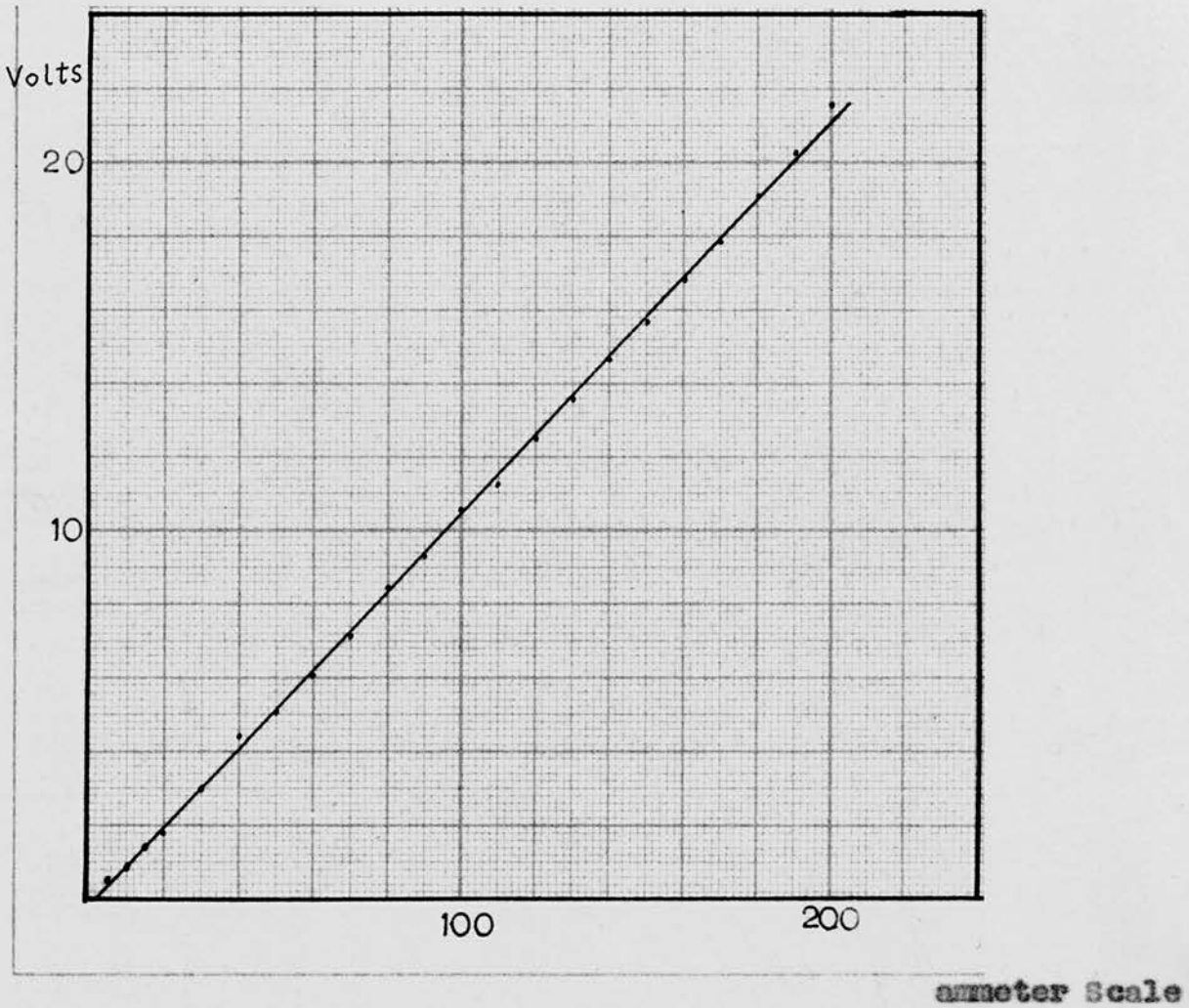

FIG. 19: 'Channel Width' Calibration Curve.

altered, but this was not appreciable compared to the errors in setting.

Delay Line: The overall time lag between the collection of the pulses at the final stages of either system could be estimated by comparing the total time necessary in each system for a single event occurring in the chamber to appear at the output. When an α-particle of about 6 MeV is emitted towards the anode in a direction perpendicular to the grid, its track R_o in argon is about 5 cm. Assuming the range-energy relation $R \propto E^{\frac{3}{2}}$ for α-particles and the energy per ion pair to be constant, it follows that the centre of gravity lies $\frac{2}{5}$ R from the end of the track (Wilkinson, 1950). The time of flight of the electrons from this point to the anode is calculated to be approximately 1.1 μsec., using the electron mobility data on the argon-methane mixture as obtained from the graphs given by English and Hanna (1953). The single channel pulse height analyser then introduces a further delay of approximately 1 μsec., giving a total delay of just over 2 μsec.

On the other hand in the Υ-detection system, the time lag between the occurrence of the ionizing event and the output pulse, caused by the transit time together with the build-up period of the scintillation

and the light collection time is of the order of 10^{-2} μsec. Thus most of the delay is caused in the α-particle detection ring. In practice the actual delay was measured by displaying α-particle pulses on a cathode ray oscilloscope triggered by photon pulses, and this time-lag was compensated by employing a delay line in the γ-particle detection system so that a coincidence unit of short resolving time could be used.

A delay line should be such that it delays a voltage pulse by the necessary amount and at the same time preserves as faithfully as possible its characteristic shape. The usual type of delay line (Elmore and Sands, 1949) is essentially a low pass filter composed of lumped capacitors and inductors in as many sections as required. In such a delay line the delay per section is $\sqrt{LC}$ and the characteristic impedance is

$$Z_C = \sqrt{\frac{L}{C}}$$

The upper cut-off frequency can be calculated from the formula

$$f_C = \frac{1}{\pi\sqrt{L \cdot C}}$$

where L is the inductance in henries and C is the capacity in farads. Two delay lines of the same characteristic impedance 100 Ω were constructed, each containing fifteen sections and giving a total delay

of about 8 μsec. These were carefully shielded from outside effects by enclosing them in an aluminium housing. The one having the less mutual inductance was found to give better shape to the output pulse and was chosen for use. The terminating resistors at each end of the line were made variable and the distortion in the pulse shape displayed on the cathode ray oscilloscope was minimised by adjusting each resistor. When properly adjusted little distortion in the pulse shape was noticeable. The delay time was varied by removing individual sections and not by tapping, as pulses tend to be reflected when tapped.

The delay line was placed between the cathode follower and the input of the main amplifier as it was preferable to place it here rather than at the output of the main amplifier for reasons of impedance matching.

Later in the experiment when a more finely adjusted delay was desired a coincidence unit type 1036C was put in the ionization chamber circuit which had a variable delay time of 1 μsec. divided into 10 sections, while the delay in the scintillation counter circuit was increased accordingly.

Finally a check had to be carried out to ensure correct matching in time between the channels and this was done by switching the delay time until the genuine coincidence rate reached its maximum.

CHAPTER IV

MEASUREMENT OF SOLID ANGLE

Introduction

When the collimator-depth to source diameter ratio is small, as is the case in the present ionization chamber, accurate determination of the solid angle subtended by the source to the collimating hole is not an easy matter. Even when this could be achieved, the slightest error in the measurement of the source diameter, collimating hole depth, or collimating hole diameter could cause a great error in the calculated value of the solid angle. The coincidence experiment, however, enables one to measure the solid angle accurately and thus to calculate the counter efficiency of the ionization chamber.

Let $N_{\alpha\gamma o}$ be the number of coincidence counts and $N_{\gamma o}$ the number of photons observed per unit time. Since for every photon from a Cm^{242} disintegration there is an α-particle emitted at the same time, the coincidence counting rate should be the same as the photon counting rate provided all the α's are detected. However, the number of α-particles actually producing ionizations in the sensitive volume of the chamber, and counted, constitute a finite fraction of the total number. Therefore we have

$$N_\alpha \Omega_\alpha = N_{\alpha o}$$

and similarly for photons,

$$N_\gamma \Omega_\gamma = N_{\gamma_0},$$

$$N_{\alpha\gamma_0} = N_\gamma \Omega_\gamma \Omega_\alpha = N_{\gamma_0} \Omega_\alpha$$

$$\therefore \Omega_\alpha = \frac{N_{\alpha\gamma_0}}{N_{\gamma_0}}$$

The effect of purely random coincidences and the background counting rate of the NaI(Tl) scintillator must be corrected for.

Random coincidences: When coincidence techniques are employed the problem of random coincidences arising from two unrelated events is always present because of the finite coincidence resolving time. This is particularly so when the number of unrelated events is comparable to or exceeds that of related events. In general, even if all the events under investigation were related, the detection efficiencies of the counters are usually so low that most of the events detected by each counter are unrelated and then the equation

$$N_R = 2(N_1 \cdot N_2)\tau \qquad (4.1)$$

is used to determine the random coincidence rate, N_R. However when the detection efficiencies are as great as in the present study of α-γ coincidences, related events become more numerous, and the above formula needs correction. Let us assume that the counting loss due to the dead time effect of each channel is negligible. We define N_R' to be the number of purely random coincidences

and N_C to be the number of genuine coincidences. Then, if we consider a pulse in channel 1 that is not related to any pulse in channel 2, the probability per unit time that this pulse should be observed in coincidence with a pulse in channel 2 appears on first sight to be $2N_2\tau$. This, however, is not correct since from the number of pulses N_2 we must subtract the N_C pulses which have already triggered the coincidence unit, producing coincidences coming into the genuine category. Thus the purely random coincidence rate N_R' is given by

$$N_R' = 2\tau(N_1 - N_C)(N_2 - N_C) \qquad (4.2)$$

This formula reduces to the correct form in both limits of (i) no genuine coincidences $N_C = 0$

$$N_R' = 2\tau N_1 N_2 \qquad (4.2a)$$

and (ii) all pulses related $N_1 = N_2 = N_C$

$$N_R' = 0 \qquad (4.2b)$$

whereas equation (4.1) does not hold for this case.

If we assume, to start with, that N_C is equal to the measured coincidence rate we can then determine N_R' from equation (4.2), thus converging on its true value by successive approximations.

In order that this procedure could be adopted, an accurate determination of the coincidence resolving time

was required. This was obtained by taking the coincidence counting rate between the pulses from two completely independent sources - Cm^{242} α-particle pulses from the chamber and Am^{241} γ-ray pulses from the scintillation counter - thus the recorded counting rate was due to random coincidences alone. As an alternative the conditions prevailing in the main experiment could be very closely simulated by introducing a long delay in the ionization chamber output and observing random coincidences between L-X-rays from Cm^{242} and unrelated α-particles from the same source. Both methods were found to give agreement within the experimental error.

The Coincidence Unit: In order to measure the solid angle subtended by the α-particle source at the collimator it was not critical which energy region was selected, subject to some uncertainty as to whether there exists any α-γ correlation.

The output from the scintillation counter was fed into an EKCO type N 568 amplifier and the output pulse passed to the channel 1 input of a Harwell type 1036C coincidence unit, the counting rate of this channel being recorded by a Type 200 scaler.

The α-particle pulses recorded by the chamber passed from the head amplifier to an N 568 linear pulse

amplifier, the maximum gain of which was 86 db. with a possible attenuation of 40 db. in steps of 2 db. It was usually set at an attenuation of 16 db. The output pulses from this amplifier were fed into channel 3 of the coincidence unit, the single channel counting rate being recorded by another Type 200 scaler. Coincidences between channels 1 and 3 were also registered by a scaler of the same type.

The delays between the crystal detector and the α-particle detector were equalized by inserting an external delay line of the type discussed above (p. 56) having a delay time of about 2 μsec. A final adjustment was obtained using the small variable delay provided in the coincidence unit until coincidences were observed. The delay time of the external delay line was determined by increasing it until the observed coincidence rate reached its maximum, while the internal delays of both channels were set equal.

Both the differentiating and integrating time constants of each amplifier were set at 0.8 μsec. for this experiment because this setting gave shorter pulses, thus favouring a shorter coincidence resolving time at the expense of a slight worsening in the energy resolution. The coincidence mixer for channels 1 and 3 of the coincidence unit had a resolving time variable

between 0.1 μsec. and 4 μsec. and the optimum coincidence resolving time was found to be 2 μsec. This was determined from the graph between the coincidence rate and the resolving time.

The multi-channel pulse height analyser could also be used to measure the solid angle (if the longer resolving time and the resulting greater number of random coincidences were not of first importance.) An advantage of using the multi-channel pulse height analyser lies in its energy selection in the L X-ray region. When L X-rays alone are used for coincidence, the question of angular correlation does not arise.

No information on the α-γ angular correlation of Cm^{242}, Cm^{243}, Cm^{244} or Pu^{238} was available, though the α-γ angular correlation of Th^{230} (Io) has been investigated by Paul Falk-Vairant (1954), who found that the emission of L X-rays following α-disintegration of Th^{230} (Io) was isotropic. Cm^{242} and Th^{230}(Io) are sufficiently alike (they are both even-even nuclei with similar simple α-disintegration schemes to make it reasonable to assume that the emission of L X-rays following the α-disintegration of Cm^{242} is also isotropic. However, in the present experiment the results obtained by the above two methods were in disagreement to the extent of about 2 % , which was about the ~~same as the~~

same as the experimental error involved in either method. Thus it could not be established whether or not any effects arose due to an α-γ correlation.

Solid Angle for Photons: The photon detector efficiency, on the other hand, could not be determined in this manner, because the statement that "every photon is accompanied by an α-particle" does not hold the other way, that is to say, the statement that "every alpha is accompanied by a photon" is not true.

However, if the source-to-crystal distance is made reasonably large (3 or 4 cm., say) and a well defined collimator (see Chapter III) is placed in front of the crystal and the source diameter is known, the solid angle can actually be calculated in terms of complete elliptic integrals of the first and third order, using the equation given by Paxton (1959),

$$\Omega = 2\pi - \frac{2L}{R_{max}} K(k) - \pi \Lambda_0(\xi, k) \qquad (4.3)$$

where

$$R_{max}^2 = L^2 + (r_0 + r_m)^2$$

$$k^2 = \frac{4 r_0 r_m}{L^2 + (r_0 + r_m)^2}$$

$$\xi = \arctan \frac{L}{|r_0 - r_m|}$$

L : The source-to-collimator distance.

r_o : The source diameter.

r_m : The diameter of the collimator

Neither inhomogeneity of the source nor inaccuracy of the source-to-crystal distance, and the diameters of the source and the collimator are not critical for the accuracy of the solid angle calculation under these circumstances.

The result of the calculation was compared with the case of a point source obtained from the approximate relation

$$\Omega = \frac{r^2}{4L^2}$$

and at a distance greater than 3 cm. the difference was found to be less than the experimental error arising from other factors.

In order to confirm the above-mentioned points an experiment was carried out in which the source-to-crystal distance was varied and the photon counting rate taken at different distances. Generally speaking the intensity of radiation from a source is inversely proportional to the square of the distance and a graph was drawn of $(\text{intensity})^{-\frac{1}{2}}$ against $(\text{distance})^{\frac{1}{2}}$, showing this relationship at various distances (Fig. 19 a). In the experiment the observed counts were first of all

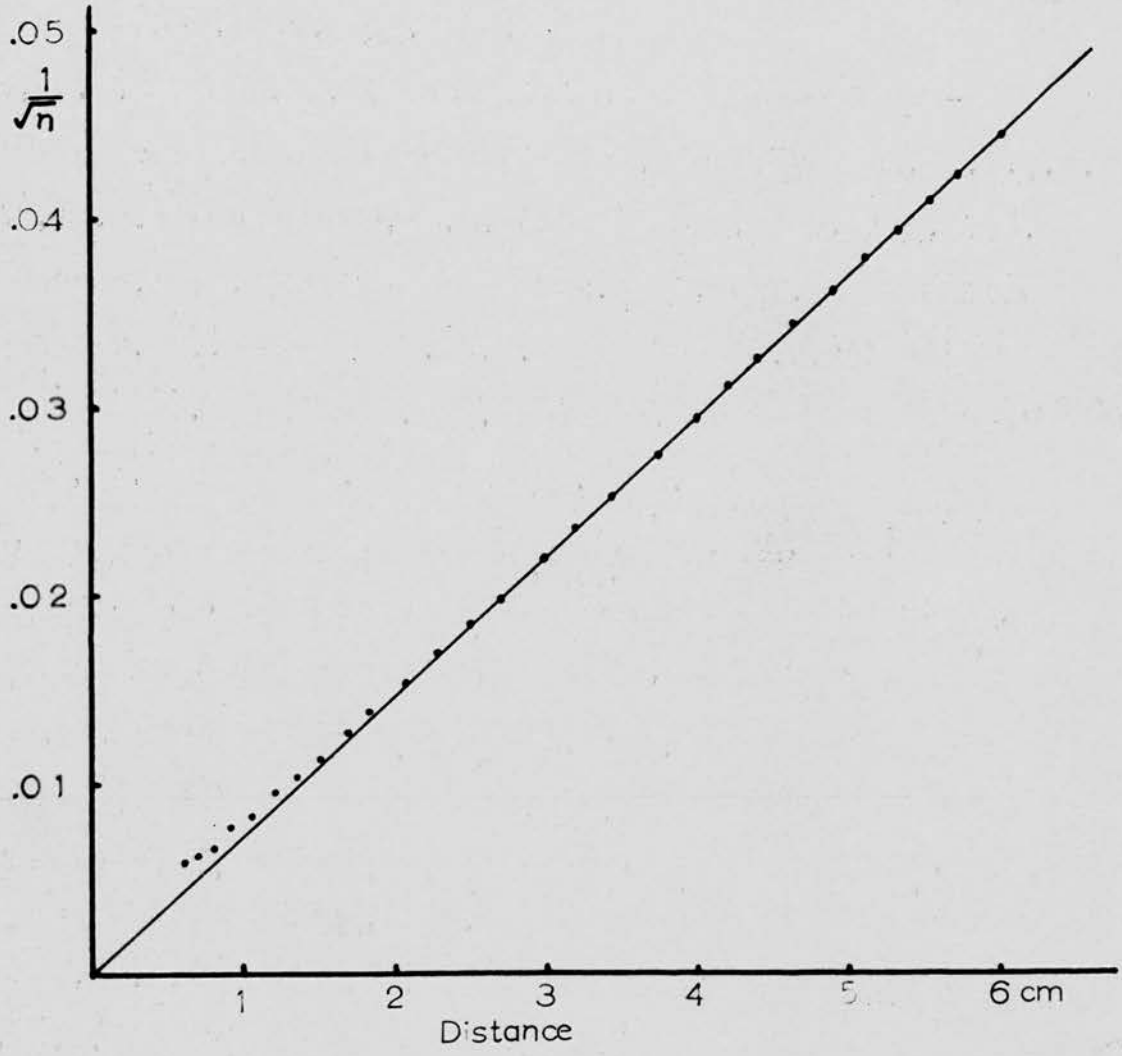

FIG. 19a: The variation of counting rate (n) with Source-to-Crystal distance.

corrected for the dead time effect and then for the background effect of the scintillation counter. No corrections were made for the different thicknesses of the air, but this was not an appreciable factor at the distances under consideration. The graph shows that at distances greater than 3 cm. the experimental curve practically coincides with the straight line passing through the origin and fitted to the points lying between the distances 3.5 cm. and 6 cm. from the source by a least squares calculation. The statistical error of all the points taken was less than 1% . In this experiment, however, the lead collimator was not fitted to the crystal and therefore a theoretical curve obtained from equation (4.3) could not be compared with this graph.

CHAPTER V

EXPERIMENTAL RESULTS

So far we have been mainly concerned with the operation of the various instruments employed in this research and with the large number of subsidiary experiments which were necessary to ensure that measurements made in the main experiment could be correctly interpreted. The emphasis placed on trying to consider every relevant factor, however minor, is justified from the fact that the experiment depends critically on the measurement of a number of absolute as opposed to relative quantities. It was also particularly necessary to guard against the possibility of obtaining spurious results arising from the fact that the recording apparatus was sensitive to events occurring simultaneously with and very similar to the particular phenomena under investigation. As is the case in most coincidence work, the experiment consists in examining a spectrum in coincidence with a second or "gating" spectrum. However, there is this difference that contrary to the usual case, it is in this "gating" spectrum that the greatest resolution is necessary. Although the determination of relative yields is one of the objects of the experiment, the scintillation counter cannot resolve the individual

X-ray lines nor indeed is this necessary and the combination of high efficiency and fast reaction time of the NaI scintillator more than compensates for the poor resolution obtained, compared with that given by, for instance, a proportional counter. Keeping these particular points in view we now go on to consider the experimental results in some detail, starting off with a discussion of some measurements made on the source.

The Source

The source of Cm^{242} used in the experiment came in the form of a thin deposit on an aluminium foil of 0.68 mg./cm^2 superficial density and was prepared by Dr. Milsted at A.E.R.E, Harwell. Just after preparation the Cm^{242} alpha activity was stated by the maker to be 1.6 μC and the total alpha-activity of Cm^{243} and Cm^{244} combined was 1.2% of the total according to the same authority. Cm^{242} has a half-life of 162.5 days, while the half-lives of Cm^{243} and Cm^{244} are 35 and 19 years respectively, so that after about two half-lives of Cm^{242} the activity of Cm^{243} and Cm^{244} isotopes had risen to about 6% of the total, by which time the alpha-activity of the daughter product ~~of~~ Pu^{238} had also become detectable. Three peaks were therefore observed in the alpha particle spectrum, a large peak due to Cm^{242} and two lesser peaks due to

Cm^{243} + Cm^{244} and Pu^{238}. There was some overlap between these peaks but in general this overlap contributed a negligibly small part of the total spectrum so it was possible during the course of the experiment to keep a check on the growth and decay of the constituent activities in the sample.

The results of a number of measurements made over the period of the work are shown in Fig. 20 and we may make some comments on them. First of all the curve of the Cm^{242} activity plotted against time is consistent within the experimental error with the value of the half-life of Cm^{242} as given in the "Table of Isotopes" (Strominger et al., 1958). The period over which measurements were made was too short however for any useful information to be obtained from the results concerning the half-lives of the longer lived nuclides Cm^{243}, Cm^{244} and Pu^{238}. As regards the growth of Pu^{238}, the experimental results have been compared with a theoretical curve based on the assumption that the activity of Pu^{238} was zero at the time of preparation, but the statistical accuracy is bad since the Pu^{238} activity is very low and effects due to scattered alpha-particles make the background correction uncertain. The decay curve of the Cm^{243} + Cm^{244} alpha-particle group is shown in the same figure, but once again poor statistics make a determination of

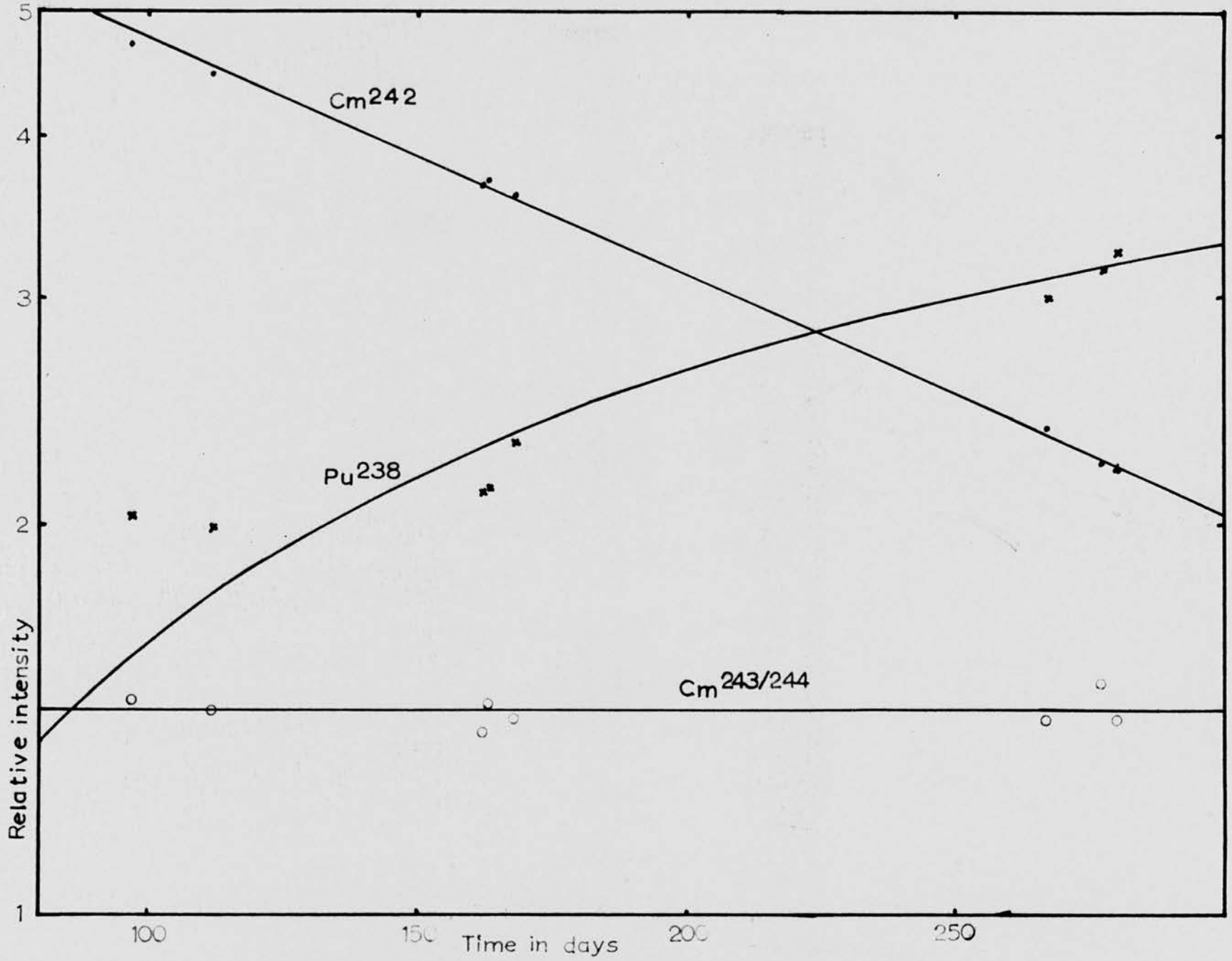

FIG. 20: Decay and Growth of Source Constituents.

the fractional composition of this group unreliable.

The presence of the Cm^{243} isotope in the source could have some consequences for the main experiment and hence it has to be very carefully considered. The type of effect it is likely to produce may be seen from the following considerations:

(i) About 10% of the alpha-particles from Cm^{243} lie under the main Cm^{242} peak and are not distinguishable from Cm^{242} alpha-particles.

(ii) Cm^{242} and Cm^{243} have very different decay schemes since Cm^{242} is an even-even nucleus, while Cm^{243} is odd(A)-even(z); moreover, far less information is available on the decay scheme of the latter. These remarks do not apply to Pu^{238} and Cm^{244}, which resemble Cm^{242} in many ways.

(iii) From a study of the information that is available in the decay of Cm^{243} it appears that up to five times as many L X-rays may appear for disintegration of this nucleus ~~than~~ as is the case for Cm^{242}. Such a large yield of L X-rays could have serious consequences and hence it becomes a matter of importance to determine the fractional amount of Cm^{243} actually present. As was noted already the growth and decay curves discussed above give no information on this point, though it should be pointed out that the fact that there is some Cm^{243} present is easily confirmed by observing in

in the photon spectrum the 226 keV and 278 keV γ-rays which follow its disintegration. The presence of these γ-rays provided the basis for one of the two methods used to determine the fraction of Cm^{243} in the source and these methods will now be considered.

(i) The pulse height from the ionization chamber is proportional to the energy of the alpha-particle and thus the total alpha-particle spectrum could be calibrated, using the Cm^{242} peak and the Pu^{238} peak as known points. In this way it was possible to determine the mean energy of the "impurity" peak and, knowing the energies of the constituent peaks, therefore to calculate the relative abundance in the peak of Cm^{243} and Cm^{244}. By this method it was found that 27% of the impurity peak was due to Cm^{243}, though the error in this determination was rather difficult to assess. In particular we might consider one reason why this is so. The probability that a Cm^{243} nucleus should disintegrate into an excited state of Pu^{239} is much greater than that a Cm^{244} disintegration should lead to an excited state of Pu^{240}. Hence the probability that a Cm^{243} alpha particle should be accompanied by an electron is much greater than for a Cm^{244} alpha particle and in addition the electrons in the former case have a much greater mean energy. The net effect is that the combined peak may be moved upwards to a

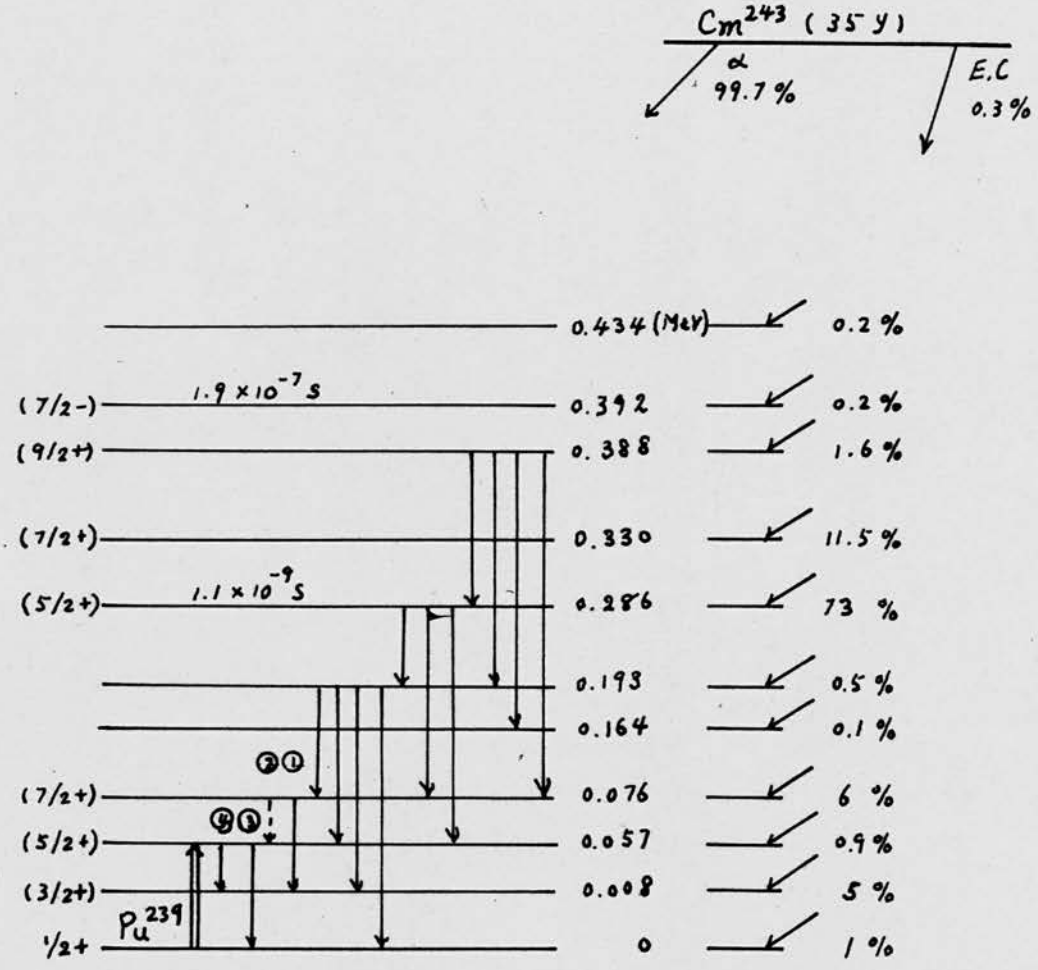

FIG. 21: Cm^{243} Decay Scheme (Strominger et al. 1958).

higher energy, thus leading to an overestimate of the Cm^{243} abundance. However, the solid angle for alpha-particle detection is so small that only about 2 % of electrons would be simultaneously observed with the alpha-particle and so it appears that the effect is hardly likely to be serious. Another difficulty however is that the energy difference of the two groups ~~are~~ is only about 11 keV and hence slight variation of the position of the impurity peak would affect the estimation of the Cm^{243} content considerably.

(ii) The second method used was to deduce the number of Cm^{243} disintegrations from a measurement of the intensity of the 226 keV and 278 keV γ-rays. Asaro ~~et al.~~ (1953) ~~have~~ has measured the absolute intensity of these γ-rays and ~~have~~ has deduced that they occur in about 30 % of all disintegrations. However, ~~their~~ his results are rather doubtful due to uncertainties in the geometrical factor for ~~their~~ his NaI crystal.

The relative intensities of the γ-rays from Cm^{243} have been measured by Newton et al. (1956) and the results are given in the table below.

Unfortunately no figure for the number of γ-rays per alpha-particle is given in this work, hence this number had to be estimated from a study of the decay scheme of Cm^{243} (Fig. 21). In Newton's paper it was

TABLE V.1.

Relative Intensities of Cm^{243} γ-rays (Newton et al., 1956)

Energy	102.15 keV	117	210	228	277
Relative Intensity	3.6	1.4	0.5	0.65	1.00

suggested that the multipolarities of the 209 keV, 226 keV and 277 keV transitions were a mixture of E2 and M1. However more recent values of internal conversion coefficients suggest that they are probably nearly pure M1 and hence their absolute intensities could be ~~calculated~~ checked with the use of Sliv's table of internal conversion coefficients, the values being 25.8 % of Cm^{243} α-disintegration. Thus a measurement was made of the intensities of these γ-rays which ~~therefore~~ gave a figure for the amount of Cm^{243} activity present when a correction had been made for the efficiency of the NaI scintillator. ~~The result, that 25% of the impurity in the source was due to Cm^{243}, was in surprisingly good agreement with the value obtained by the earlier method and the accuracy of the estimates is quite sufficient for this purpose.~~

See Appendix in envelope inside back cover.

Experimental Value of $N_{\gamma c}/N_{\alpha}$

With this information and a knowledge of the alpha-particle spectrum of Cm^{243} and our observed spectrum we are now in a position to conclude that the following α-rays from Cm^{243} make some contribution to the main "Cm^{242}" peak - 6.061 Mev (0.016%), 6.054 Mev (0.08%), 6.005 Mev (0.014%) and 5.987 Mev (0.064%) where the intensities are expressed as a percentage of the total Cm^{242} α-intensity in the peak. We must now calculate the number of L X-rays which should be observed in coincidence with these Cm^{242} alpha-particles. peak. The 6.061 Mev transition to the ground state cannot of course produce any L-rays and neither can the 6.054 Mev transition to the excited state 7 keV above the ground state since the energy of the following γ-ray is too low. Thus only the transitions to the 57 keV and 76 keV excited states can produce any relevant effect. From an examination of Fig. 21 we can see that when spin changes are taken into account the only transitions from the 76 keV excited state which are important are the transitions marked (1) and (2) in the diagram and these are likely to be E2 and MI respectively. Both these transitions are forbidden and so rated as the relative probabilities of their occurrence as far as the fourth power of the energy difference between them. Thus it can be seen

that the E2 transition is completely dominant and the M1 transition may be neglected. In the de-excitation of the 57 keV level however the energy difference between the competing modes (3) and (4) is very small and we may take it that they are equally probable . With this estimate and with the help of Sliv's (1958) values for the internal conversion coefficients the total L X-ray yield following Cm^{243} disintegration in the above mentioned energy groups was calculated to be of the order of 2.9% of the total number of Cm^{243} α-disintegrations and hence the observed Pu^{238} L X-ray intensity could be corrected.

When all the corrections so far discussed were made, the values of the L X-ray intensity per α - disintegration as obtained in two experiments were:

$$F/N_{\alpha}^{N_{Lc}}$$

Experiment 1.	0.0980 $\pm$ (0.9%)
Experiment 2.	0.0945 $\pm$ (2.6%)
Weighted Average	0.0971 $\pm$ (0.74%)

Although the final result was obtained from only two experimental values the consistency of the experimental results was checked many times. Other results are not included above because of difficulties which

arose, in the selection of Cm^{242} alphas as gating pulses for the coincidence unit. The reliability of the coincidence count can be judged from a comparison of (a) and (b) in Fig. 22, where it is seen that the pulse height distribution in the coincidence spectrum and the total spectrum of L X-rays are very similar. The majority of the background counts in the total spectrum are not observed in the coincidence spectrum, while the remaining part of the background is taken into account when the random coincidence correction is made.

All that remains now for the calculation of the fluorescence yields is to determine the quantities C_3 , $\alpha(L) / \alpha(\Sigma)$ and F_3 defined earlier (p. 19), for which purpose recourse must be had to the published work of others.

Values of C_3 and $\alpha(L)/\alpha(\Sigma)$

$\alpha(L)$ and $\alpha(\Sigma)$ have been obtained experimentally by Passell(1954), Smith and Hollander (1956), and Baranov and Shlyagin (1956), and theoretically by Rose (1958) and by Sliv and Band (1958). Although Smith and Hollander used two very high resolution spectrometers their data on relative intensities is rather unreliable since the photographic recording

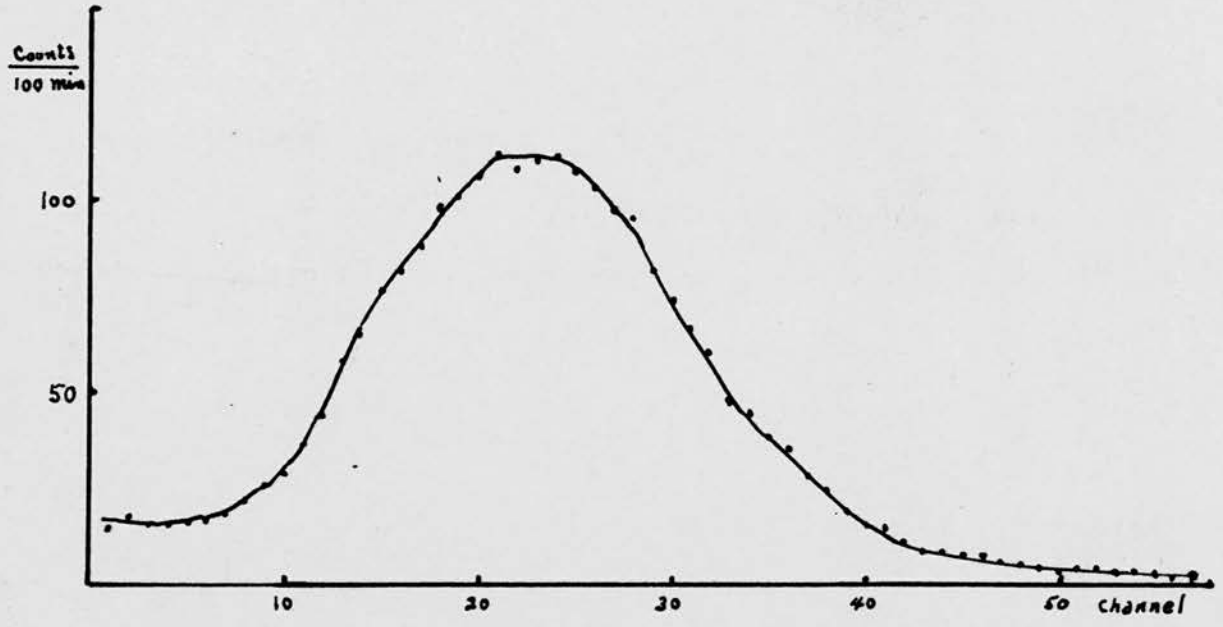

FIG. 22a: Spectrum of L X-rays in Coincidence with Cm^{242} Particles.

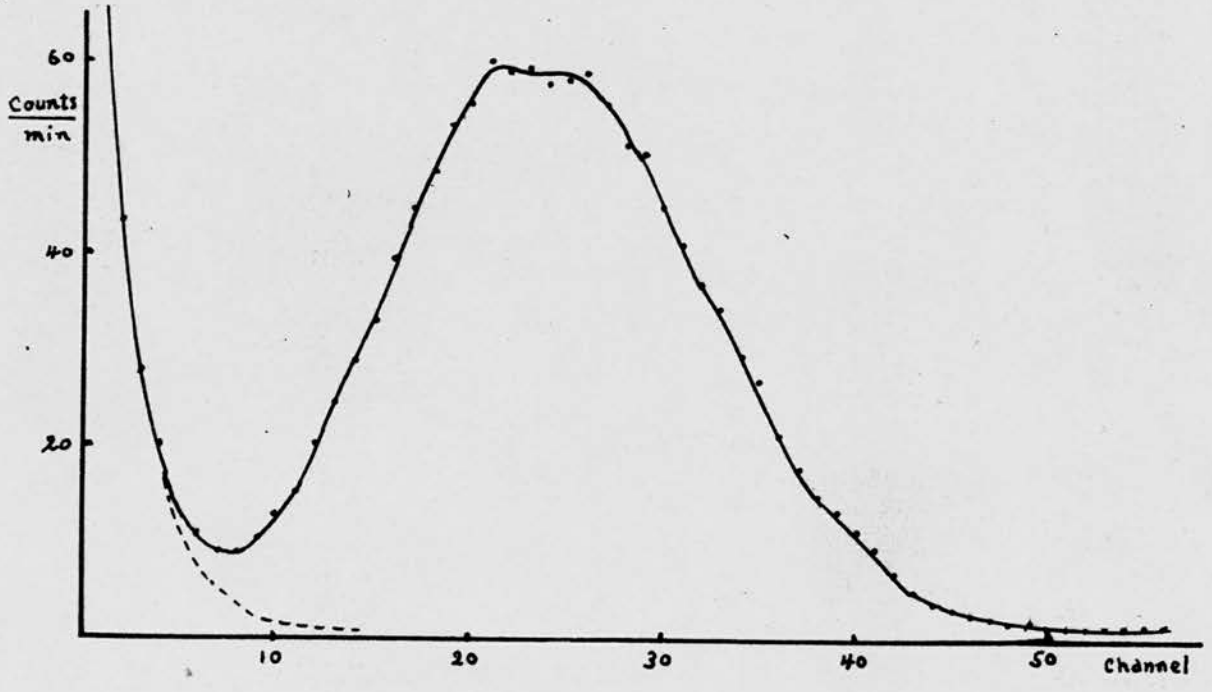

FIG. 22b: Total Spectrum of L X-rays (no coincidence gating).

was used in their work and the sensitivity of photographic plates depends in a rather uncertain fashion on the electron energy. On the other hand, Baranov and Shlyagin did not have sufficient resolution available, their background was high and they did not specify what recording device they used. In the work of Passell the internal conversion peaks in the L_{II} and L_{III} subshells and the M shell for 44 keV γ-rays from Cm^{242} and Np^{238} are well resolved. However on the low energy sides of the L_{II} and L_{III} conversion peaks in the Cm^{242} spectra there is a high background and thus the Np^{238} results have been accepted as being the more reliable. Thus from these data the ratios $\alpha(L)/\alpha(\Sigma) = 0.773$ and $\alpha(L_{III})/\alpha(L_{II}) = C_3$ $C_3 = 0.795$ have been determined. A comparison with the theoretical results of Rose for $\alpha(L)/\{\alpha(M) + \alpha(L)\}$ $= 0.682$ shows that Rose's figures are somewhat less, which is not very surprising as the finite size of nucleus was not taken into account in his calculations. There is better agreement with the results of Sliv and Band for C_3, although they give no figures for M-shell conversion and hence it is not possible to calculate $\alpha(L)/\alpha(\Sigma)$ from their data. However the ratio of the conversion coefficients in the L and M shells is usually about 3 and the result of 2.7 obtained from Passell's measurements is quite consistent with this.

Value of F_3

As the crystal scintillator does not have sufficient resolution to separate out the Plutonium L X-rays which follow on the disintegration of Cm^{242}, we are forced to rely again on results taken elsewhere with instruments of higher resolution. For the L X-ray spectrum following the Cm^{242} disintegration itself we have the results of Barton et al. (1951) and Ferreira (1956), both workers having obtained their data using bent crystal X-ray spectrometers. As before, detection was by photographic film and the same questions arise regarding the sensitivity of the film when relative intensities are concerned. Added to this is the question of how the crystal reflectivity varies with incident X-ray energy and, taking into account these two objections, it is not surprising that there are considerable discrepancies between the results of the two groups. However, it does seem that we should be able to accept the result for those lines whose energy difference is small and this is confirmed from the fact that the figures from two groups agree fairly well for such lines. It seems therefore that combining this information with that on neighbouring elements in a wider range of Z-values given by Jöhnsson (1926) and Allison (1928) as quoted in Compton and Allison (1935) we should be able to arrive at an

TABLE V.2

Relative Intensities of L X-ray Lines of Pu following Cm^{242} α-disintegration.

Line	Transition	Energy (KeV)	Intensity (Relative)		
			Barton et al.	Ferreira	Compton & Allison (Deduced value)
ℓ	$L_{III} - M_{I}$	12.13			3.99
α_2	$L_{III} - M_{IV}$	14.08	13	13.2 ± 1.9	11.14
α_1	$L_{III} - M_{V}$	14.28	100	100 ± 4.5	100
β_6	$L_{III} - N_{I}$	16.50	-	-	1.39
β_2	$L_{III} - N_{V}$	17.25	28	25 ± 1.3	23.20
β_7	$L_{III} - O_{I}$		-	-	0.33
β_5	$L_{III} - O_{V}$	17.95	6	4.8 ± 0.5	5.11
η	$L_{II} - M_{I}$	16.32	-	-	3.97
β_1	$L_{II} - M_{IV}$	18.27	91	106 ± 4.6	86.24
γ_1	$L_{II} - N_{IV}$	21.38	23	21.4 ± 0.7	17.87
γ_6	$L_{II} - O_{IV}$	22.13	4	3.9 ± 0.4	3.18

accurate value for the relative intensities. We are mainly interested in the L_{II} and L_{III} subshells and so the relative intensities for X-rays from these shells are tabulated in Table V.3 where the intensities are corrected to the number of photons rather than the ionization intensities as given in Compton and Allison's original table. It should be noted that the figures for the relative intensities of lines originating from different subshells cannot be applied in our work, since the method of excitation used is different. However the relative intensities of line coming from the same subshell should be the same. Hence the following procedure has been adopted. From Table V.2 we can see that Barton's results and Ferreira's results are in close agreement for the β_1 and β_2 lines and so we can use the ratio of the β_1 intensity to the β_2 intensity as a measure of the ratios of the initial number of vacancies in the L_{II} and L_{III} subshells. The β_1 and β_2 lines are good for this purpose since (i) their energies lie close together, and (ii) their intensities are reasonably high. Combining this result with the figures in Table V.3 for relative intensities of line originating in the same subshell, we may arrive at a value for the relative intensities of the total number of X-rays originating in the L_{II} and L_{III} subshells respectively. The final value obtained in

TABLE V.3

Relative Intensities of L Group Lines Obtained by Fluorescent Excitation

Line	Transition	W (Jonsson)		Th (Allison)		U (Allison)	
		Energy	Intensity	Energy	Intensity	Energy	Intensity
ℓ	$L_{III} - M_I$	7.388	3.64	11.117	44.20	11.619	3.99
α_2	$L_{III} - M_{IV}$	8.335	11.62	12.810	12.15	13.442	11.14
α_1	$L_{III} - M_V$	8.398	100	12.968	100	13.617	100
β_6	$L_{III} - N_I$	9.611	0.974	14.976	1.21	15.729	1.39
β_2	$L_{III} - N_V$	9.961	6.88	15.623	21.58	16.430	23.20
β_7	$L_{III} - O_I$	10.130	-	16.009	0.32	16.843	0.33
β_5	$L_{III} - O_V$	10.170	0.168	16.212	4.95	17.071	5.11
η	$L_{II} - M_I$	8.725	1.252	14.509	1.61	15.397	1.8
β_1	$L_{II} - M_{IV}$	9.672	45.20	16.202	44.612	17.221	39.07
γ_5	$L_{II} - N_I$	10.948	0.3111	-	-	-	-
γ_1	$L_{II} - N_{IV}$	11.285	6.708	18.980	9.57	20.166	8.10
γ_6	$L_{II} - O_{IV}$	11.507	0.2186	-	-	20.849	1.44

this factor for F_3 was 1.26 which can be compared with Barton's value of 1.24 and Ferreira's value of 1.09. The calculations following have been based on the assumption that 1.26 is the correct figure.

Value of F/I.

The total fluorescence yield F/I can be obtained from equation (1.15), which can be put in the form

$$\frac{F}{I} = \frac{N_{\gamma c}}{N_a} \cdot \frac{1 + \frac{1}{\alpha(\Sigma)}}{0.263 \times \frac{\alpha(L)}{\alpha(\Sigma)}} \qquad (5.1)$$

The factors $\frac{N_{\gamma c}}{N_a}$ and $\frac{\alpha(L)}{\alpha(\Sigma)}$ are known and

$\frac{1}{\alpha(\Sigma)} = \frac{1}{\alpha(L)} \frac{\alpha(L)}{\alpha(\Sigma)}$. We use Sliv's value $\alpha(L) = 596$ to calculate $\frac{1}{\alpha(\Sigma)}$ and since $\alpha(\Sigma)$ is large, it only enters as a small term in the numerator of (5.1) and so any small error in Sliv's value for $\alpha(L)$ will have a negligibly small effect on F/I. The result obtained is

$$\frac{F}{I} = 0.478 \pm 0.015$$

ω_2, f_{23}, a_2 and a_3 are determined from equations (1.8), (1.9), (1.10) and (1.11), using a value of $\omega_3 = \overset{0.455}{\cancel{45.5\%}}$ obtained by a least square extrapolation of the data for 11 elements given by Küstner and Arends (1935), Stephenson (1937) and Kinsey (1948a).

Errors

Although the error in the quantity actually measured in the present experiment is only about .74% the errors in the values obtained for the fluorescence yield will be considerably larger than this. Calculation of the errors in the quantities obtained from the work of others is rather difficult, since the limits of error are not given in most of the original papers. Thus the best that can be done is to compare all the available results and arrive at an estimate of the error in this fashion.

C_3. The experimental values for C_3 range from .694 to .991 and the latter limit obtained from Baranov's Np spectrum may be discarded since the high background in his spectrum made accurate calculation of C_3 almost impossible. From the remaining data we conclude that the value we have accepted is correct to within $\pm$ 3.8 % which is generous in that it covers most of the experimental values and gives fairly close agreement with the best (Sliv's) theoretical value available. In any case, the point is not very critical in that the resultant error in ω_2 is only about 1 % .

F_3. There is less information available for F_3 than for C_3. Fereira's value for F_3 is less than the value we use, which agrees closely with that obtained by Barton and it appears reasonable to assign an error

of about 2.4 % to our value. The corresponding error in the value of ω_2, derived from this, is about 1.2 % . F_3 and C_3 make about equal contributions to the error in f_{23} and since f_{23} is the difference between two much larger numbers the error in it is very big and is estimated to be about 42 % .

$\frac{a(L)}{a(\Sigma)}$. This is a quantity which must be very carefully considered since it is the dominant factor in the determination of both $\omega = F/I$ and ω_2. Both the values obtained from the work of Passell (1954) and Slätis (1954) are covered if an accuracy of $\pm$ 2.5 % is assigned to the value that we use here, though the values of Smith and Hollander and Baranov and Shlyagin lie outside these limits. The reasons why their work has been ignored are given earlier and in any case they were more concerned with energy measurement than with intensity measurement. Thus we take it that $\frac{a(L)}{a(\Sigma)}$ is correct within the limits of accuracy given above.

ω_3. This quantity has been the subject of about twenty investigations, spread over some eleven elements, and it is found by an examination of the literature that all these determinations are in agreement to the extent of about 2 % . This is not surprising since ω_3 is a reasonably easy number to measure and its

determination is to a large extent independent of auxiliary information. Thus we have assumed our value of ω_3 to be correct within the limits of about 2% .

Having introduced these estimated errors into our equations, we are now in a position to give the final result for the quantities we originally set out to determine. These results are:

$$\omega_2 = 0.38 \pm 0.03$$

$$f_{23} = 0.26 \pm 0.12$$

$$a_2 = 0.36 \pm 0.15$$

$$a_3 = 0.55 \pm 0.01$$

Discussion and Conclusion

Some of the results given above are compared in Table V.4, with results from other sources on neighbouring heavy elements, though the information available for elements in the region of Z = 94 is very scanty. Kinsey's values were obtained by an indirect method, based on the comparison of radiation widths and under the assumption that $f_{23} = 0$. However this assumption may not hold in the region of $Z > 90$, when $L_{II} - L_{III}$ M_{IV}, M_V transitions are possible and thus his results are not of great value to us for comparison purposes. Cochran's (1955) values on U and Np were obtained by measuring

TABLE V.4

The Values of the Yields in L_{II} and L_{III} Shells

Element	Th	U		Np	Pu
Yields	(Kinsey)	(Kinsey)	(Cochran)	(Cochran)	(Present Work)
ω_2	0.56	0.59	0.30 ± 0.04	0.35 ± 0.06	0.38 ± 0.03
ω_3	0.39	0.41	0.46 ± 0.02	0.46 ± 0.02	0.45 ± 0.01
f_{23}	-	-	0.40 ± 0.3		0.26 ± 0.12

the relative intensities of L X-rays from three sub-shells, assuming $f_{12} = 0$, and his value for F/I was taken from Lay's (1934) experiments, and C_2 and C_3, which relate to the initial vacancies, were obtained from the absorption jump ratios.

Although there is more information on Z = 81 and 83, there is little point in comparing them with the present results for the reasons that (1) a sudden jump in the value of f_{23} exists at Z = 90 and, (2) the values actually given for the yields for these elements are inconcistent.

It is now quite apparent that the only useful comparison that can be made is between Cochran's value for ω_2 in Neptunium and our own value for ω_2 in Plutonium, and there is clearly no inconsistency between the two results. It can also be said that although the limit of error is large in the value of f_{23}, the presence of an appreciable amount is very well proved. Apart from this the following general conclusions may be drawn.

(i) The whole field of the L-shell fluorescence yields suffers from a lack of experimental information and it is quite obvious that a large amount of work remains to be done before the situation may be considered as satisfactory.

(ii) Not only is information lacking, but much of it that is available is unreliable and this can be

traced to the fact that most of the experiments done depend for their final results on auxiliary information obtained from other sources. In many cases an abundance of such information exists which is, to a large extent, self-contradictory so that it becomes largely a matter of chance which items are accepted as being correct.

(iii) It is believed by the writer that the results of measurements actually made in this experiment are correct and reliable, though the final results suffer from the uncertainties noted in (ii) above however careful and selective one may be in the assessment of material available in the literature of the subject. For this reason a considerable amount of thought has been put to devising an experiment for the determination of the L-shell fluorescent yields which would produce all the desired information at once and thus be independent of doubtful results obtained elsewhere. An outline of an experiment to determine ω_3, which it is believed, conforms essentially to these ideas, is presented in the appendix.

APPENDIX

Proposed Measurement of ω_3 in a Wider Range of Z

Introduction

The existing data on ω_3 has been compiled by Burhop (1952) and the averaged values from the work of Küstner and Arends (1935), Stephenson (1937) and Kinsey (1948a) have been taken to exhibit the agreement between the experimental values and the theoretical expression of Burhop and Massey (1936)

$$\frac{\omega_{L_{III}}}{1 - \omega_{L_{III}}} = a_{L_{III}} Z^4$$

where $a_{L_{III}}$ is a constant. The values available however were limited to only eleven elements and moreover in many cases, only one figure was available for a given element and not a single element was investigated by all three groups. Thus it appears that the process of averaging is not really justified, since under these circumstances a systematic error in the work of one individual may seriously affect the entire scheme. If instead of plotting a curve of $\frac{\omega_{L_{III}}}{1 - \omega_{L_{III}}}$ against Z^4 for the average of the three groups, three separate plots are made (Fig. 23) an interesting feature appears in that, within each group the points lie on clearly defined curves, however the nature of these curves are all quite different. Thus it seems that the confirmation of the theoretical expression by the experimental

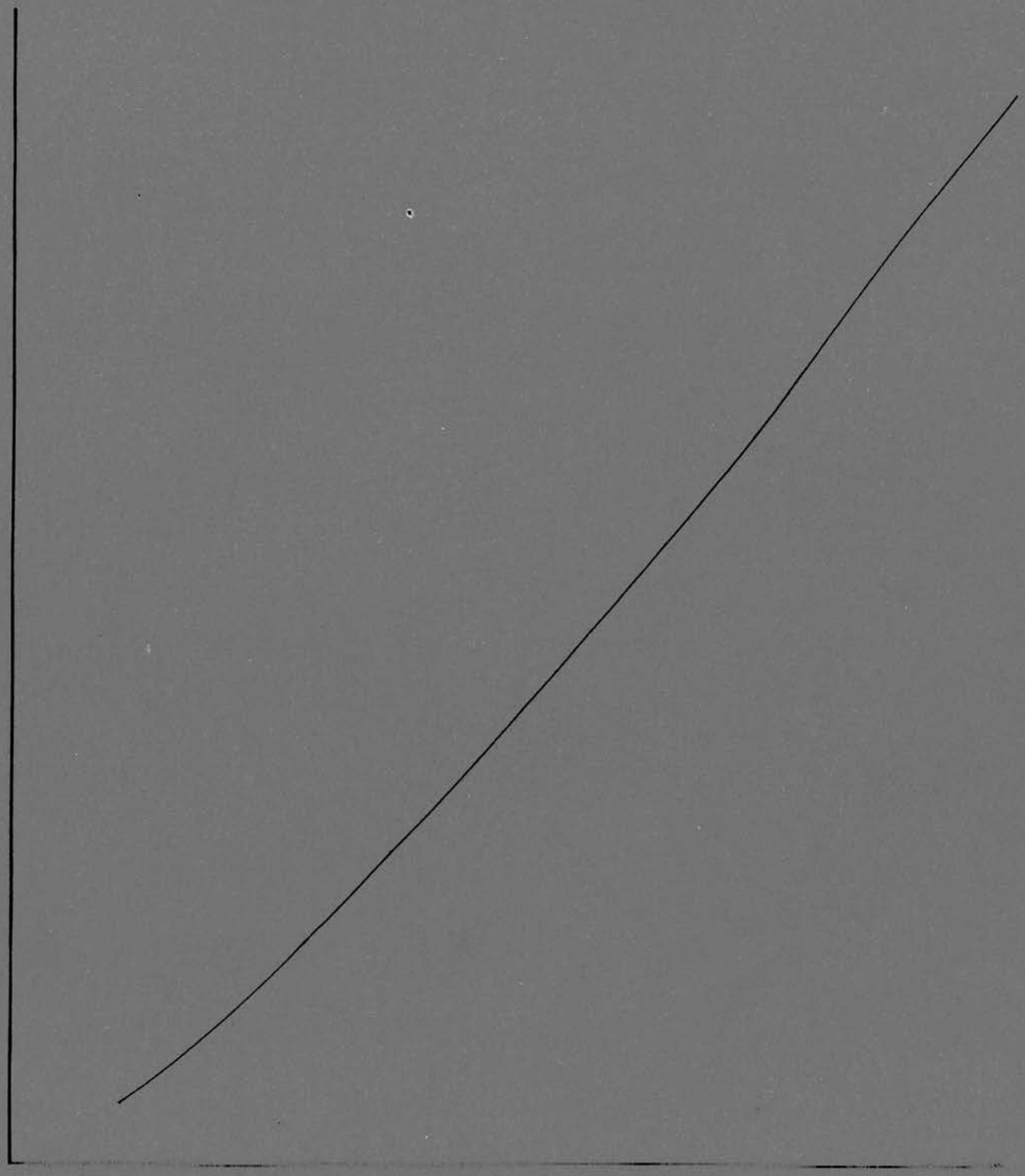

FIG. 23a

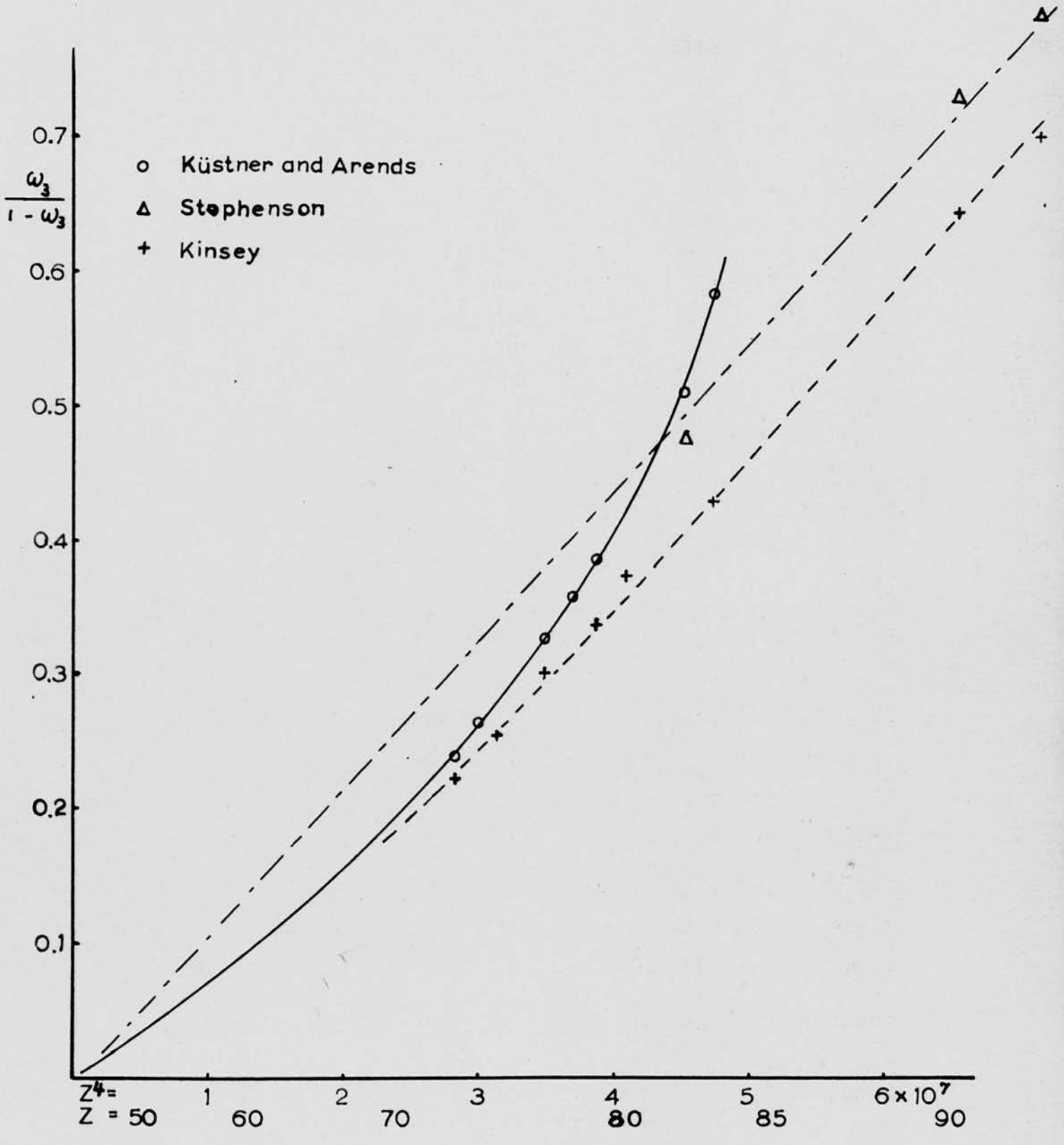

FIG. 23: The Variation of $\omega_3/(1-\omega_3)$ with Z^4.

results so far available is doubtful and in particular, if the results of Küstner and Arends are correct the theoretical law is not confirmed. However, when the screening correction which has a greater effect in the L shell than in the K shell is taken into account, the values of Küstner and Arends can be made to agree with the theory for values of $\omega_{L_{III}}$ in the range of $Z < 80$. The theoretical law, including the screening effect, is

$$\left(\frac{\omega_{L_{III}}}{1 - \omega_{L_{III}}} \right)^{\frac{1}{4}} = A + BZ$$

and this is also shown in the figure (Fig. 23a) for comparison purposes, the constants A and B being obtained from Burhop's (1955) calculations. Although Kinsey's values seem to be in better agreement with the later theory the data are not sufficient at this stage to confirm the theory completely. Thus we can only conclude that there is no real agreement on the experimental side concerning the true values for ω_3 and that a systematic investigation of this problem would be quite a valuable contribution to the field as a whole.

The Method

In arriving at a method for the determination of ω_3 free from the limitations mentioned earlier, there

are two main factors to be considered: (i) the form of excitation, and (ii) the type of detector. As regards the first factor fluorescent excitation is preferred to the use of radioactive samples, since it reduces to a minimum the amount of auxiliary information required and is far more flexible in that it places a far wider range of elements at one's disposal for investigation. In selecting a detecting and measuring system it seems reasonable to examine the possibilities offered by the methods used for determining the K-shell fluorescence yields, which were reviewed in the first chapter. These may be recalled briefly under the following headings:

(i) Cloud chamber

(ii) Magnetic Spectrometer

(iii) Ionization chamber

(iv) Solid Angle Difference Method

(v) Proportional Counter.

Method (i) is immediately ruled out for the reason that great skill and experience are needed to distinguish the low energy tracks and also it is difficult to acquire good statistics. (ii) is rejected for the reason that, using fluorescent excitation, it does not offer any easy means of determining with accuracy the number of initial vacancies. The use of ionization

chambers as in (iii) would require that different samples be used to obtain the absorption coefficients of the element under investigation for the exciting and for the fluorescent radiation. One could use the published X-ray absorption data, but it is of course desired that the determination be independent as far as possible of outside sources of information. The same kind of considerations apply to method (iv), although it is a much better method in that the same part of the sample foil could be used for both the absorption and fluorescence measurements and that the detecting efficiency for the secondary radiation is very high, and hence a scheme based on the use of a proportional counter (V) has finally been considered.

If two identical proportional counters are placed side by side to form a double counter with the sample placed between them in a hole in their common wall, and a collimated beam of X-rays of suitable energy is used to excite the fluorescence, then the total number of initial vacancies produced in the sample may be calculated by measuring the counting rate for exciting X-rays in both counters and the initial intensity of the X-ray beam. The latter measurement can easily be made with a scintillation counter. Furthermore, if the energy of the X-ray beam is carefully selected to

lie between the L_{II} and L_{III} levels, then vacancies can occur only in the L_{III} level and a measurement of the counting rate for fluorescent X-rays in both counters, suitably corrected for escape effects, will give the fluorescent yield for the L_{III} shell. The energy resolution available from a proportional counter would be quite sufficient to resolve out the parts of the observed spectrum due to the exciting X-rays and the fluorescent X-rays respectively. Even allowing for the extra spread in the pulse spectrum due to the occasional simultaneous observation of an M X-ray it would be necessary to shield off the counters from all Auger or photo-electrons coming from the sample.

It might be noted that it is possible to allow for any slight differences in the characteristics of the two counters by reversing the direction of the exciting beam in a repeat experiment.

This is the principle of the proposed experiment. However, it is further suggested, for reasons to be given below, that the double counter be made from one circular cylinder with a plane through the axis of the cylinder, to form the dividing wall. Thus each counter would have a semi-circular cross section, as shown in Fig. 24, though, provided the position of the wire were carefully chosen, it does not appear that the

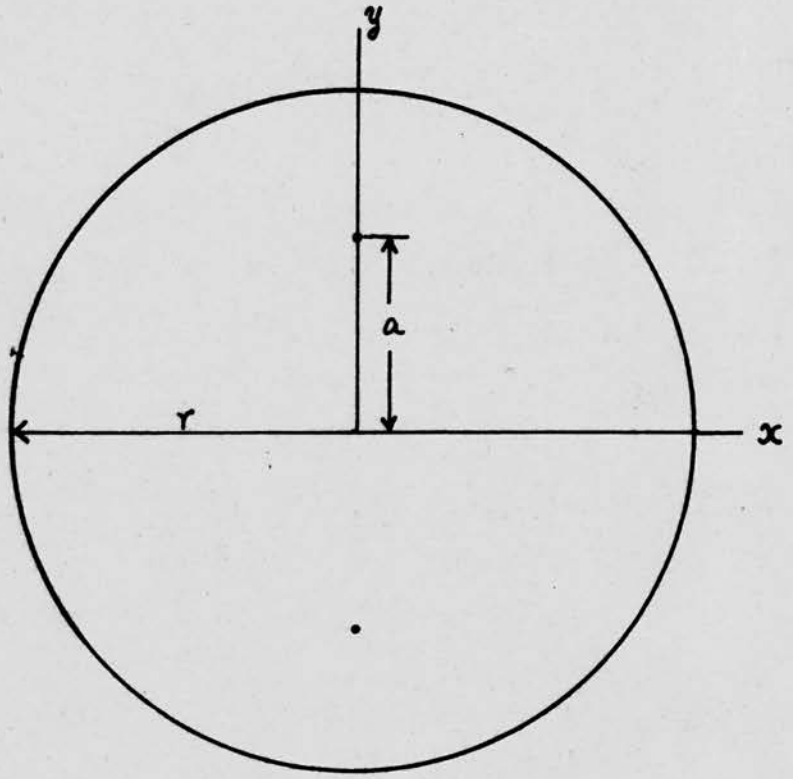

FIG. 24: Proposed Double Proportional Counter for the Measurement of ω_3.

rather peculiar geometry should have any adverse effect on the operation of the device as a proportional counter. This is true for the reason that in a proportional counter the amplifying effect only takes place in a region very close to the wire, so that provided the field strength is sufficient, at all points in the counter to prevent recombination of electrons and ions, the actual form of the field is only of importance in the region of the wire. The potential problem posed by such a geometry may be solved by the method of images, as calculated by Mr. J. Byrne of this Department, and the equations of the equipotential s referred to axes through the centre of the cylinder are given by

$$\frac{\{x^2 + y(y + b) + r^2\}^2 + x^2(2y + b)^2}{\{x^2 - y(y + b) + r^2\}^2 + x^2(2y - b)^2} = \text{const.}$$

where r is the radius of the cylinder.

a is the distance of the wire from the dividing wall and

$$b = \frac{r^2 - a^2}{a} .$$

It can easily be shown that in the region close to the wire, these equipotentials become circles to a very good approximation if $a = \frac{r}{\sqrt{3}}$ and under these circumstances the pulse height produced by the counter

the most novel aspect of the arrangement arises from the fact that the exciting beam of X-rays may be incident on the sample from any angle without upsetting the equality of the counting rate for fluorescent X-rays in either counter. The only difference that one might expect at angles away from the normal would be a slight increase in counting rate, due to the extra path in the sample traversed by the exciting X-ray beam. However if there were any angular correlation between the exciting and fluorescent X-ray quanta, such a correlation should be quite apparent as a periodic difference in counting rate between the two counters when the source of exciting X-rays is rotated through the full circle.

ACKNOWLEDGEMENT

I wish to express my sincere gratitude to Professor N. Feather, F.R.S., for extending to me the facilities of his laboratory and for the continued interest he has taken in the course of this research.

I am deeply indebted to Dr. M.A.S. Ross for suggesting the subject of this thesis and for her advice and encouragement throughout the work and also to Dr. J. Muir for many helpful discussions and suggestions.

I am also indebted to Dr. Milsted of The Atomic Energy Research Establishment, Harwell, for the provision of the Curium source.

I should also like to acknowledge the help and cooperation given to me by Mr. Headridge and his staff in the workshop of the Department of Natural Philosophy.

Finally I am indebted to the Office of Atomic Energy, of the Republic of Korea for the provision of a Scholarship Award during the first two years of this research, and to the W.D. Brodie Memorial Fund for a further grant which enabled me to complete the work.

.....

BIBLIOGRAPHY

Alfven, H. (1935) Nature, London, 136, 70.

Allison, S.K. (1928) Phys. Rev. 32, 1.

Asaro, F. (1953) Thesis, University of California, UCRL 2180.

Arends, E. (1936) Ann. Phys. 22, 281.

Asaro, F., Thompson, S.G. & Perlman, I. (1953) Phys. Rev. 92, 694.

Auger, P. (1925) J. Phys. Rad. 6, 205.

Backhurst, I. (1936) Phil. Mag. 22, 737.

Baranov, S.A. & Shlyagin (1956) J. Nuclear Energy 3, 132.

Barkla, C.G. & Sadler, C.A. (1909) Phil. Mag. 17, 739.

Barton, G.W., Jr., Robinson, H.P. & Perlman, I. (1951) Phys. Rev. 81, 208.

Bearden, J.A. & Snyder, T.M. (1941) Phys. Rev. 59, 162.

Beatty (1911) Proc. Roy. Soc. A85, 230.

Bergstrom, I. & Thulin, S. (1950) Phys. Rev. 79, 539.

Bertolini, G., Bettoni, M. & Bisi, A. (1954) Nuovo Cimento, 11, 458.

Bohr, A. (1954) Rational States of Atomic Nuclei, Thesis, Copenhagen.

Broyles, C.D., Thomas, D.A. & Haynes, S.K. (1953) Phys. Rev. 89, 715.

Buneman, O., Cranshaw, T.E. & Harvey, J.A. (1949) J. Canad. J. Res. 27, 191.

Burhop, E.H.S. (1935) Proc. Roy. Soc. A148, 272.

Burhop, E.H.S. (1952) 'The Auger Effect', Cambridge University Press, Cambridge.

Burhop, E.H.S. (1955) J. Phys. Rad. 16, 625.

BIBLIOGRAPHY (Contd.)

Cochran (1955) Thesis, University of Edinburgh.

Compton, A.H. & Allison, S.K. (1935) X-rays in Theory and Experiment (Van Nostrand), p. 645.

Cooper, J.N. (1942) Phys. Rev. 61, 234.

Coster, D. & Kronig, L. (1935) Physica 2, 13.

Cottini, C., Gatti, E., Giannelli, G. & Rozzi, G. (1956) Nuovo Cimento III, 473.

Cranshaw, T.E. & Harvey, J.A. (1948) Canad. J. Res. A26, 243.

Curran, S.C., Angus, J. & Cockroft, A.L. (1949) Phil. Mag., 40, 36.

Elmore, W.C. & Sands, M. (1949) Electronics. New York, (McGraw Hill Book Co.)

English & Hanna (1953) Canad. J. Phys. 31, 768.

Falk, P., Vairant, J.T., Valladas, G. & Mme. P. Benoist (1954) Compt. Rend., 2381, 1409.

Ferreira (1956) Unpublished data, private communication.

Frisch, O.R. As quoted by Clark, F.L., Spencer-Palmer, H.J. & Woodward, R.N. J. of South African Chem. Inst., X, 62 (1957).

Gerbes, W. (1935) Ann. d. Phys. 23, 648.

Germain, L.S. (1950) Phys. Rev. 80, 937.

Gray, L.H. (1944) Proc. Camb. Phil. Soc.

Gray, P. R. (1956) Phys. Rev. 101, 1306

Harrison, G.R., Crawford, R.C. & Hopkins, J.I. (1955), Phys. Rev. 100, 841.

Johnsson, A. (1926) Z. Phys. 36, 426.

BIBLIOGRAPHY (Contd.)

Kinsey, B.B. (1948a) Canad. J. Res. 26, 404.

Kinsey, B.B. (1948b) Ibid., 26, 421.

Kustner, H. & Arends, E. (1935) Ann. Phys. Lpz., 22, 443.

Laberrigue-Frolow, J. & Radvanyi, P. (1956) J. Phys. Rad. 17, 944.

Lay, H. (1934) Z. Phys., 91, 533.

Livingston, M.S. & Bethe, H.A. (1937) Rev. Mod. Phys., 9, 266.

Martin, L.H. (1927) Proc. Roy. Soc. (London) A115, 420.

Massey, H.S.W. & Burhop, E.H.S. (1936) Proc. Camb. Phil. Soc., 32, 461 (or Proc. Roy. Soc. A153, 66)

Newton, J.O., Rose, B. & Milsted, J. (1956) Phil. Mag. 1, 981.

Nijgh, G.J., Wapstra, A.H. & Van Lieshout, R. (1959) Nuclear Spectroscopy Tables, p. 82.

Park, E.C. (1956) J. Sci. Inst., 33, 257.

Passell, T.O. (1954) Thesis, University of California, Rad. Lab. Rep. UCRL-2528.

Paxton, F. (1959) Rev. Sci. Inst. 30, 254.

Pilger (R.C.). (1957) Thesis, University of California, UCRL 3877.

Pincherle (1935) Nuovo Cimento, 12, 81.

Richtmyer, F.K., Barnes, S.W. & Ramberg, G. (1934), Phys. Rev. 46, 843.

Robinson, H.R. & Young, C.L. (1930) Proc. Roy. Soc. A128, 92.

Roos, C.E. (1954) Phys. Rev. 93, 401.

Roos, C.E. (1957) Phys. Rev. 105, 931.

Rose, M.E. (1958) Internal Conversion Coefficients. (North Holland Publishing Co.)

Ross, M.A.S., Cochran, A.J., Hughes, J. & Feather, N. (1955) Proc. Phys. Soc., 68, 612.

BIBLIOGRAPHY (Contd.)

Sherr & Peterson (1947) Rev. Sci. Inst., 18, 567.

Slater, J.C. (1930) Phys. Rev. 36, 57.

Slätis, H., Rasmussen, J.O. Jr., and Atterling, H. (1954) Phys. Rev. 93, 646.

Sliv, L.A. & Band, I.M. Coefficient of Internal Conversion of Gamma Radiation, Acad. of Sci. U.S.S.R.

Smith, W.G. & Hollander, J.M. (1956) Phys. Rev. 101, 746.

Stephenson, R.J. (1937) Phys. Rev. 51, 637.

Strominger, D., Hollander, J.M. & Seaborg E.T. (1958) Rev. Mod. Phys. 30, 585-904.

Wentzel, G. (1927) Z. Physik 43, 524.

West, D. & Rothwell, P. (1950) Phil. Mag. 41, 873.

Wilkinson, D.H. (1950) Ionization Chambers and Counters. (Cambridge University Press, Cambridge).

An estimate was required of the error introduced into the observed value of F by the ^{243}Cm contamination of the source. If the number of gating pulses from ^{242}Cm and ^{243}Cm are respectively $N_{\alpha 1}$ and $N_{\alpha 2}$ and the numbers of coincident L X-ray photons are N_{X1} and N_{X2} then $F = N_{X1}/N_{\alpha 1}$ and $F_{obs} = (N_{X1} + N_{X2})/(N_{\alpha 1} + N_{\alpha 2})$.

From a knowledge of the decay scheme of ^{243}Cm (Fig. 23) and of the observed line shape in the α-particle spectrum, the fraction of all ^{243}Cm α-particles which lay within the gating group was estimated to be 11.8 %. L-shell vacancies would be produced in about 0.37 of these cases, the corresponding fraction for ^{242}Cm being 0.203. The total intensity of ^{243}Cm α-particles was estimated from the observed intensity of the 226 and 278 keV γ-ray lines which have been shown by Asaro (1953) to arise from ^{243}Cm and to have a total intensity of 0.30 per disintegration of the parent nucleus. Taking account of the efficiency of crystal detection and the angular apertures for photons and α-particles in the experiment, it was found that 85 α-particles per minute out of a total of about 21000 per minute in the gating group were attributable to ^{243}Cm.

Now $N_{\alpha 2}/N_{\alpha 1} = 85/20915$ and $N_{X2}/N_{X1} = 0.37N_{\alpha 2}/0.203N_{\alpha 1}$ so that

$$F_{obs} = 1.003\ F.$$

The correction is clearly so small that further refinement in relation to sub-shell effects is unnecessary.

The discriminator determining the minimum size of pulse entering the gating circuit was set to accept all α-particles from ^{242}Cm and reject as many as possible from ^{243}Cm. No upper limit was set to the pulse size. The adjustment of the discriminator was correct when the rate of counting of the gating pulses was equal to the known rate of counting in the ^{242}Cm peak.

The observations used for the measurement of F are shown in table 4. For each experiment the total observed count is shown followed by the duration of the observation in minutes (shown in brackets). Counts were taken for all gating pulses ($N\alpha$), all photons ($N\gamma$), and for all L X-ray photons in coincidence with ^{242}Cm α-particles (N_x). Beneath each observed count the corrected counting rate per minute is shown. Dead time corrections were applied to all counts and correction for random coincidences to N_x. The weighted mean of the values of F is 9.31 ± 0.1 .

The mean correction for absorption of the L X-rays in the path between source and crystal was evaluated knowing the absorption coefficients and the superficial density of each material traversed. The efficiency of the crystal was taken as unity. The resulting mean correction factor was 1.067. The resulting mean value of F after correcting for the contamination by ^{243}Cm was 9.905 ± 0.1.

Table 4. Data for the evaluation of F

(Time of observation in minutes is shown in brackets. Corrected counts per minute are shown beneath the uncorrected observations.)

N_α	N_γ*	N_x	$\Omega_\gamma/4\pi$	F
211145 (10)	90395(100)	996 (80)	0.005160	9.226
21151.7 (1)	914.16 (1)	10.070 (1)		
530881 (25)	as above	2467 (200)	0.005160	9.057
21272.9 (1)		9.942 (1)		
355943 (17)	as above	13100(1060)	0.005160	9.237
20974.4 (1)		9.998 (1)		
415878 (20)	74004 (50)	25109(1000)	0.010879	9.385
20830.0 (1)	1507.64(1)	21.267 (1)		

* This count is required for dead time and random coincidence correction and it is therefore uncorrected for background counts (which were about 282/min.).